SOIL SALINITY AND FEATURE CLASSIFICATION USING ARTIFICIAL NEURAL NETWORK

by

BRIJESH KUMAR RAI

CE
1997
M
RAI
SOI

DEPARTMENT OF CIVIL ENGINEERING

INDIAN INSTITUTE OF TECHNOLOGY KANPUR

March, 1997

SOIL SALINITY AND FEATURE CLASSIFICATION USING ARTIFICIAL NEURAL NETWORK

A thesis submitted
in partial fulfilment of the requirements
for the degree of

MASTER OF TECHNOLOGY

by
BRIJESH KUMAR RAI

to the

DEPARTMENT OF CIVIL ENGINEERING
INDIAN INSTITUTE OF TECHNOLOGY, KANPUR

MARCH, 1997

24 APR 1997 / CE

Acc. No. A 123313

CE-1997-M-RAI-SOI

CERTIFICATE

Certified that the work presented in this thesis entitled **"Soil Salinity and Feature Classification using Artificial Neural Network"** by **Mr. Brijesh Kumar Rai** (Roll. No. 9510310) has been carried out under my supervision and has not been submitted elsewhere for any degree.

March 27, 1997

Nitin Tripathi

(Nitin Kumar Tripathi)
Assistant Professor
Geoinformatics
Department of Civil Engineering
Indian Institute of Technology
Kanpur

DEDICATED TO MY PARENTS

ACKNOWLEDGEMENT

I feel pleasure in expressing my most sincere gratitude to Dr. Nitin Kumar Tripathi for his valuable guidance, academic liberty and constant encouragement throughout the course of this work. His clear deep insight into many problems encountered during the period of work enable me to accomplish the task. His ever helping attitude and extremely encouraging remarks made me feel at home at I.I.T. Kanpur. The memories of working with him will be cherished all along my life.

I am very much grateful to Dr. Onkar Dikshit for his unforgettable help at every stage during my stay at IITK. I am also grateful to Dr. B. C. Raymahashay and other faculty members, whose lectures and guidance developed some essential capabilities in me to perform this work.

I am grateful to P. K. Kalra for his advice and providing me basic material for this work. I received a big help from Dr. D. N. Sharma, Professor and Head, Department of Soil Salinity, CSAU for providing me salinity data of study area.

Without the financial support of CSIR, this work could never have been under taken. Thanks to them for providing me Junior Research Fellowship at IITK.

Thanks are due to Mr. G. P. Mishra, who always acted as guardian and I found him very near at every stage of my difficulty. Thanks are also due to Mr. Ramkrishen.

I am thankful to all my friends who have made my stay memorable and indispensable part of my life. Special thanks to Neeraj, SP, Sudhir, Ravi, Tapan, Vivek, Rajesh, Bijay, Vishvanath, Venkat, Pradeep, Sameer, Pankaj, Ajay and Pandu.

Brijesh Kumar Rai

CONTENTS

		PAGE
LIST OF TABLES		iv
LIST OF FIGURES		viii
ABSTRACT		
CHAPTER 1	INTRODUCTION	1-1
	1.1 General	
	1.2 Study Site and Data Resources	1-3
	1.3 Computational Platforms for the Study	1-6
	1.3.1 Hardware used	1-6
	1.3.2 Software Details	1-7
	1.4 Objective and Scope	1-7
	1.5 Organisation of the Work	1-7
CHAPTER 2	BACKGROUND OF WORK	2-1
	2.1 Unsupervised Classification	2-2
	2.2 Supervised Classification	2-6
	2.2.1 Network input	2-7
	2.2.2 Network architecture	2-8
	2.2.3 Training algorithm	2-9
	2.2.4 Comparisons to conventional classifiers	2-12
	2.3 Summary of Classification Review	2-13
	2.4 Soil Salinity	2-14
CHAPTER 3	ARTIFICIAL NEURAL NETWORK IN IMAGE CLASSIFICATION	3-1
	3.1 Introduction	3-1

	3.2 The Biological Prototype	3-2
	3.3 Artificial Neural Network	3-3
	3.4 Input and Output Patterns	3-4
	3.4.1 Processing elements	3-4
	3.4.2 PE Functions	3-4
	3.5 Cluster Analysis and Unsupervised Learning	3-5
	3.5.1 Self Organising Feature Map (SOFM)	3-6
	3.5.1.1 Algorithm of SOFM	3-7
	3.5.1.2 Kohonen's Self Organising Feature Maps	3-9
	3.6 ANN as a Classifier	3-9
	3.7 Backpropagation Learning Algorithm	3-12
	3.7.1 The Generalised Delta Rule	3-12
	3.7.2 Eqations	3-13
	3.7.3 Limitations of the Backpropagation Algorithm	3-14
CHAPTER 4	STATISTICAL CLASSIFIERS	4-1
	4.1 Unsupervised Classification	4-1
	4.2 Supervised Classification	4-3
CHAPTER 5	CONVENTIONAL AND NEURAL CLASSIFIERS: A COMPARISON	5-1
	5.1 General	5-1
	5.2 Unsupervised Classification	5-1
	5.3 Supervised Classification	5-7
	5.3.1 Algorithm and software	5-8
	5.3.2 Configuring the network	5-10
	5.4 Training Set	5-12
	5.4.1 Training samples	5-14
	5.5 Result and Discussion	5-14

5.6 Training Accuracy for Backpropagation Classifier 5-17
5.7 Training Accuracy for MLC 5-19
5.8 Test Accuracy for MLC 5-21
5.9 Test Accuracy for ANN 5-23
5.10 Comparison of Different Classes 5-25
5.11 Comparison of Supervised Classifier 5-28

CHAPTER 6 SOIL SALINITY USING GIS AND ANN 6-1
6.1 Introduction 6-1
6.2 Probable Cause of Salinity in the Region 6-3
6.3 Type of Soil Alkalinity 6-3
6.4 Sampling Sites 6-4
6.5 Methodology 6-5
6.5.1 Soil moisture content 6-5
6.5.2 Chemical analysis 6-7
6.6 Results of Laboratory Tests 6-7
6.7 Digital Enhancement of Saline Zones 6-11
6.7.1 Digital smoothing 6-11
6.7.2 Arithmetic Operation 6-12
6.8 False Color Composites 6-14
6.9 Empirical Models using Soil Alkalinity and Spectral Reflectance 6-15
6.10 Delineation of Salinity Zones using ANN 6-19
6.11 Zones of Salinity in the Region 6-21

CHAPTER 7 CONCLUSIONS AND FUTURE RECOMMENDATIONS 7-1

REFERENCES

APPENDIX

LIST OF TABLES

Number	Title	Page
2.1	Summary of the data encoding techniques and neural structure	2-10
2.2	Summary of the times required to reach the error criterion for backpropagation training.	2-14
2.3	Summary of accuracy of different algorithms	2-15
3.1	An Algorithm to produce Self - Organising Feature Maps	3-11
3.2	The Back-Propagation Learning Algorithm	3-15
3.3	Performance measures and parameters for different neural architectures	3-16
3.4	Well- know learning algorithms	3-16
4.1	Unsupervised Clustering algorithm	4-2
5.1	Confusion Matrix for unsupervised clustering for test image	5-5
5.2	Confusion Matrix for SOFM for test image	5-5
5.3	Comparison of accuracy	5-5
5.4	Comparison of accuracy of best five classes	5-6
5.5	Area of different classes in classified images	5-7
5.6a	Confusion Matrix for Backpropagation classification of training image for 25 pixels in training for each class	5-17
5.6b	Confusion Matrix for Backpropagation classification of training image for 50 pixels in training for each class	5-17
5.6c	Confusion Matrix for Backpropagation classification of training image for 75 pixels in training for each class	5-18
5.6d	Confusion Matrix for Backpropagation classification of training image for 100 pixels in training for each class	5-18

5.6e	Confusion Matrix for Backpropagation classification of training image for 150 pixels in training for each class	5-18
5.6f	Confusion Matrix for Backpropagation classification of training image for 200 pixels in training for each class	5-19
5.7a	Confusion Matrix of Maximum Likelihood Classifier of training image for 25 pixels in training for each class	5-19
5.7b	Confusion Matrix of Maximum Likelihood Classifier of training image for 50 pixels in training for each class	5-19
5.7c	Confusion Matrix of Maximum Likelihood Classifier of training image for 75 pixels in training for each class	5-20
5.7d	Confusion Matrix of Maximum Likelihood Classifier of training image for 100 pixels in training for each class	5-20
5.7e	Confusion Matrix of Maximum Likelihood Classifier of training image for 150 pixels in training for each class	5-20
5.7f	Confusion Matrix of Maximum Likelihood Classifier of training image for 200 pixels in training for each class	5-21
5.8a	Confusion Matrix of Maximum Likelihood Classifier of test image for 25 pixels in training for each class	5-21
5.8b	Confusion Matrix of Maximum Likelihood Classifier of test image for 50 pixels in training for each class	5-21
5.8c	Confusion Matrix of Maximum Likelihood Classifier of test image for 75 pixels in training for each class	5-22
5.8d	Confusion Matrix of Maximum Likelihood Classifier of test image for 100 pixels in training for each class	5-22
5.8e	Confusion Matrix of Maximum Likelihood Classifier of test image for 150 pixels in training for each class	5-22
5.8f	Confusion Matrix of Maximum Likelihood Classifier of test image for 200 pixels in training for each class	5-22
5.9a	Confusion Matrix of Backpropagation of test image for 25 pixel	5-23

	in training for each class	
5.9b	Confusion Matrix of Backpropagation of test image for 50 pixel in training for each class	5-23
5.9c	Confusion Matrix of Backpropagation of test image for 75 pixel in training for each class	5-24
5.9d	Confusion Matrix of Backpropagation of test image for 100 pixel in training for each class	5-24
5.9e	Confusion Matrix of Backpropagation of test image for 150 pixel in training for each class	5-24
5.9f	Confusion Matrix of Backpropagation of test image for 200 pixel in training for each class	5-25
5.10a	Percentage accuracy of training image for different set of sample by Backpropagation	5-25
5.10b	Percentage accuracy of training image for different set of training sample by Maximum Likelihood classifier	5-25
5.10c	Percentage accuracy of test image for different set of training sample by Maximum Likelihood classifier	5-26
5.10d	Percentage accuracy of test image for different set of training sample by Backpropagation	5-26
5.11	Mean for training set data	5-28
5.12	Standard Deviations for training set data	5-28
5.13	Confusion matrix for classification by Backpropagation algorithm for training data	5-28
5. 14	Confusion matrix for classification by Maximum Likelihood classifier for training data	5-29
5.15	Confusion matrix for classification by maximum Likelihood classifier for test data	5-29
5.16	Confusion matrix for classification by Backpropagation algorithm for test data	5-29
5.17	Comparison of accuracy for different classes and total accuracy	5-30

	for different classifier	
5.18	Area of different classified images	5-30
5.19	Table for comparison of each class by MLC and Backpropagation classifier	5-30
6.1	Description of the sampling zones	6-5
6.2	Physical and Chemical properties of Soil Samples	6-8
6.3	Grey level values and other parameter for sampling stations (Nov, 1992)	6-9
6.4	Grey level values and other parameter for sampling station (April, 1993)	6-10
6.5	Ranking of different band compositions based on OIF value	6-15
6.6	Regression parameter to empirical modeling	6-16
6.7	Area of different saline zones using different empirical models of IRS - 1B data	6-22
6.8	Area of different salinity zone by ANN	6-22

LIST OF FIGURES

Figure	Title	Page
1.1	Land Use Land Cover Map and Sampling sites in study area	1-4
1.2	Original Band 3 image of study area	1-5
1.2	Original Band 4 image of study area	1-5
4.1	Supervised Approach of Classification using the Maximum Likelihood Classifier	4-4
5.1	FCC of study area	5-2
5.2	Classified image by unsupervised clustering	5-2
5.3	Classified Image by SOFM	5-3
5.4	Comparison of accuracy of different classes and total by unsupervised classifier	5-6
5.4	A flow chart Backpropagation Learning	5-9
5.6	ANN network for present study	5-13
5.7	Comparison of accuracy for different set of training samples of training image	5-27
5.8	Comparison of accuracy for different set of sample set of test image	5-27
5.9	Classified Image by MLC	5-31
5.10	Classified Image by BPL	5-31
5.11	Comparison of accuracy of different classes for test data	5-32
6.1	FCC of November 1992	6-6

6.2a	Empirical relationship in Spectral Reflectance in Band 3 and Alkalinity for April 1993	6-17
6.2b	Empirical relationship in Salinity Index 3 and Alkalinity for April 1993	6-17
6.2c	Empirical relationship in Normalized Difference Salinity Index and Alkalinity for April 1993	6-17
6.3a	Empirical relationship in Spectral Reflectance in Band 3 and Alkalinity for November 1993	6-18
6.3b	Empirical relationship in Salinity Index and Alkalinity for November 1993	6-18
6.4	BPL network for salinity level	6-20
6.5	BPL network for high salinity	6-20
6.6	Alkalinity map of band 3	6-23
6.7	Alkalinity map of SI	6-23
6.8	Alkalinity map of NDSI	6-24
6.9	Salinity level using ANN	6-25
6.10	Very high salinity zones	6-25

ABSTRACT

The potentials of Artificial Neural Network (ANN) has been explored for classification of IRS - 1B multispectral image. Two types of ANN approach : Self-Organising Feature Map and Back Propagation Learning have been employed for feature classification and results have been compared with conventional statistical classifiers : Unsupervised Clustering (UC) and Maximum Likelihood Classifier (MLC). The study reveals that Backpropagation Learning (BPL) has yielded better results than other classifiers.

It has been applied to extract salinity affected zones from the satellite image of Rural environs of Kanpur. A similar study using GIS and spatial / modelling has been carried out better delineation of salinity results both the approaches are compared. It is found BPL could delineate different levels of salinity in the region which are validated through results obtained using visual interpretation and field verification.

The results offered by Back Propagation Learning in feature classification encouraging and assert its superiority over Self-Organising Feature Map, Unsupervised Classifiers and Maximum Likelihood Classifier. BPL also has established to be an efficient tool for delineation of saline zone and generation of database for GIS.

CHAPTER 1

INTRODUCTION

1.1 General

Remote Sensing is generally defined as the technology of measuring the characteristic of an object or surface from a distance. In the case of Earth resource monitoring the object or surface is on the land mass of the Earth or on the sea and the observing sensor is in the air or in space. The carrier of the information to the sensor from object is Electro Magnetic Radiation (EMR) (Belward and Valenzuela, 1990). The absorption or reflectance of EMR by any material therefore varies with wavelength. It is therefore found that the reflectance and the emissivity of an object can vary with wavelength and that the variation is related to the properties of the material composition of that object. The spectral properties of major earth surface feature in different wavelength are most frequently available information to the user of remote sensing. The remote sensing satellite system provides global and repetitive coverage of Earth surface. The most important aspect of satellite remote sensing is actually identification of surface features by quantitative means. Digital image classification is a key application of remote sensing for it enable thematic maps of land feature to be created.

The purpose of *digital image classification* is to construct thematic maps where each pixel in the scene is assigned to a particular class of objects by name, based on spectral response. The objective of pattern recognition and classification is to distinguish between different types of pattern. Classification essentially is to assign input data into one or more of prespecified classes based on extraction of significant features or attributes and the processing or analysis of these attributes. The methods of image classification are based on the principle of digital pattern recognition. A digital pattern is a meaningful regularity in the data, and identification of the pattern enables classification of the data point. In remote sensing, we deal with a large amount of data lying in multidimensional space and therefore the use of computer techniques is essential. Patterns are recognised by man-machine combination.

Artificial Neural Network (ANN) is an attempt to simulate the performance of the human brain in the field of information processing. In past several studies have established ANN as a powerful tool for image classification and clustering. The massively parallel nature of ANN allows the computations at many nodes to be carried out completely independently of each other. Moreover, the transfer functions used typically are non-linear in nature, and are suitable for analog Very Large Scale Integration (VLSI) implementation. A simulation of ANN in present-day serial computers fails to make use of its massive parallelism and support for analog VLSI implementation. However, the other advantages of ANN enhance its implementation even with serial computers. Among the various ANN models developed and implemented for image classification, the multilayer perceptron is the most widely used network.

ANN holds the potential for improving a variety of tasks in remote sensing and image processing. They represent a fundamentally different approach to problems like pattern recognition, as they do not rely on statistical relationships. ANN classifiers outperform conventional classifiers mainly due to their lack of assumptions about normality in data sets. A comparative study of conventional and ANN classifier is presented in present study with special emphasis on soil salinity.

Soil salinity is one of the major problem frequently observed on fields. It hampers the land use for both, agricultural purposes as well as for many civil engineering use. Identification of salt affected area and its extent is very important for planning any structure or land use of that area. It also poses a threat to crop production as most of areas are lying barren. Salt present in soil reacts with construction materials and reduces their strength and life. To reclaim such soil for agriculture or any other purpose, the information on the nature, extent and spatial distribution of these soils is essential. In present study, identification of soil salinity is attempted by spatial modelling and ANN.

1.2 Study Site and Data Resources

Having a broad idea about the nature and appearance of saline land on the imagery, an area consisting of large number of saline patches is chosen using Lands imagery (MSS)of path no. 145 and row no. 42 on a scale 1:250,000. The approximate location of the area is determined from corresponding topographic sheet obtained from Survey of India. The chosen area, with an aerial extent about 340 sq. km is bound between $26^0 32^l$ N to $26^0 43^l$ N and $80^0 2^l$ E to $80^0 18^l$ E and forms part of the vast Indo-Gangetic alluvial plains covering part of Kanpur district of Uttar Pradesh, India.

The study area, comprising part of the Indo-Gangetic alluvium of Pleistocene age (Dwivedi et. al. 1992), physiographically is a plain with local variations such as paleochannels, oxbow lakes, minor depressions and sand dunes along the rivers and streams. Topography of the area is flat with gentle slope. The river Ganga drains the north-eastern periphery of the area, Non nadi traverse central to eastern part on both sides of the Lower Ganga Canal (Kanpur Branch). The area is irrigated by this canal and many other distributaries and minor channels. Ground water table in general is high and water quantity is good. The climate of the area is semi-arid, sub-tropical and monsoonal type. Water in abundance is available for irrigation in this region. The Map of study area is shown in Fig. 1.1.

To know various details of the area regarding ground truth such as topography, village and other features, topographic map obtained from Survey of India are used. Topographic map No. 63 B on a scale 1:250,000 is used for global perception of prominent feature of the region. For further details, a topographic map No. 63 B/2 on a scale 1:50,000 is utilised. Sampling sites are chosen based on the extensive field visits and verifying extent of salinity.

From the Indian remote sensing satellite reference map. path and row number of the study area are obtained as 26 and 49 respectively. IRS-1B LISS II satellite data is chosen for the present study. The original image of band 3 and band 4 are presented in Fig. 1.2 and

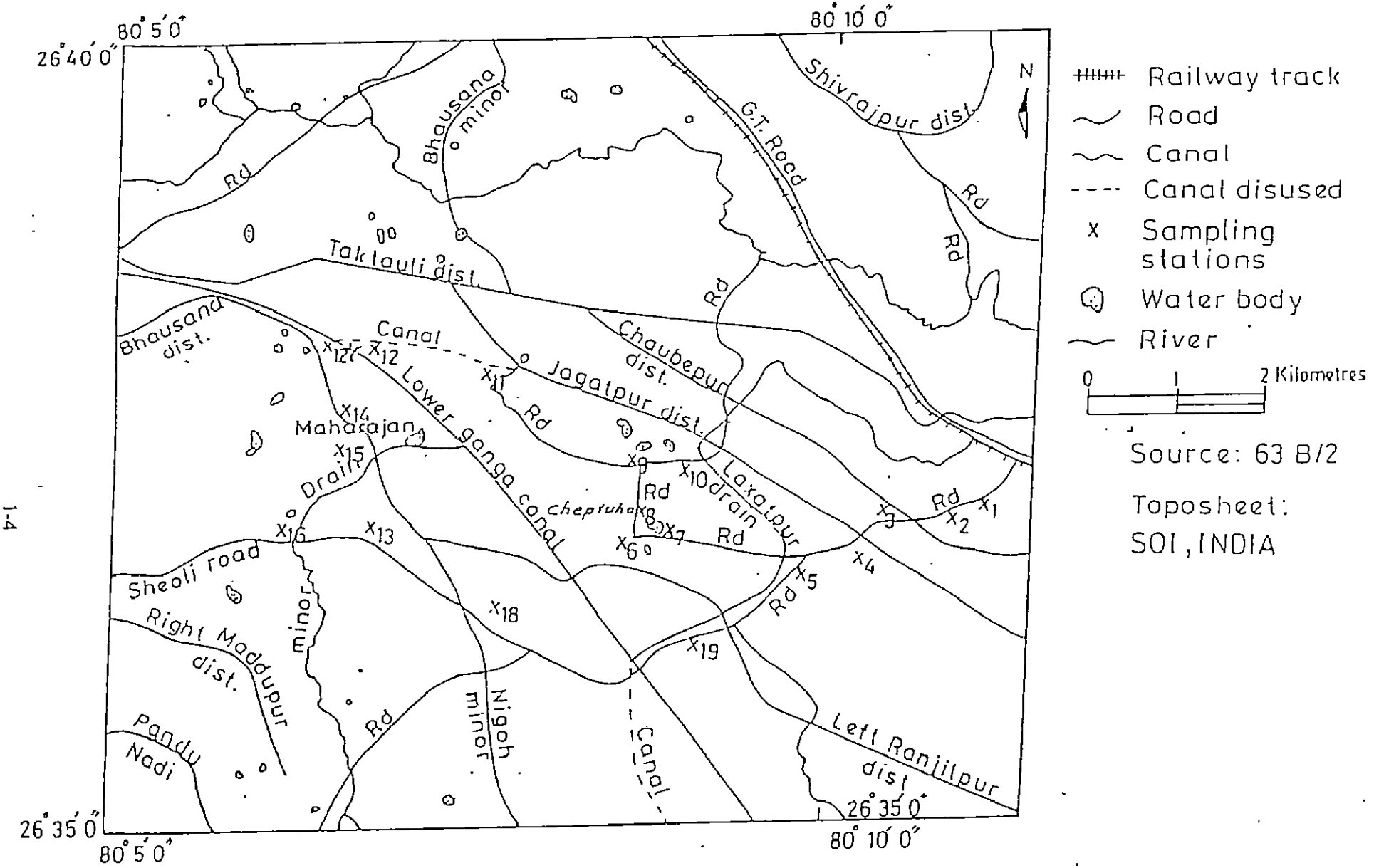

Figure 1.1: Land Use and Land Cover map and sampling sites in the study area.

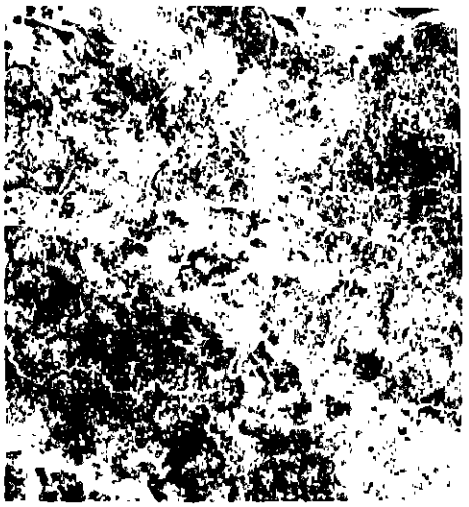

Figure 1.2: Original Band 3 image of study area

Figure 1.3: Original Band 4 image of study area

1.3 respectively. IRS-1B is Sun-synchronous satellite orbiting at an altitude of 904 km. It contains three sensors: one of LISS-I and two of LISS-II. Its repetitive cycle is 22 days and total number of bands are four as listed in Table 1.1.

To observe and monitor changes in the extent of saline zones and vegetation, digital data of two periods namely, November 1992 and April 1993 is obtained. These particular months are chosen because of their being best periods for studying soil salinity as concluded in earlier studies (Rao et. al. 1991, Dwivedi, 1992).

Table 1.1: The IRS Spectral Bands and Application

Band	Spectral Range (μm)	Principal Applications
1	0.45 - 0.52	Sensitivity to sedimentation, deciduous / coniferous forest cover discrimination
2	0.52 - 0.59	Green reflectance of healthy vegetation
3	0.62 - 0.68	Sensitivity to chlorophyll absorption, differentiation of soil and geological boundary
4	0.77 - 0.86	Sensitivity to green biomass and in vegetation, land and water contrast

1.3 Computational Platforms for the Study

1.3.1 Hardware used

All programs have been develop on the HP - 9000/735 series, locally called "Agni" and for using graphics, the HP - 9000/330 series workstations have been used. The standard hardware configuration of the system includes PC 486 DX2 66 MHz, SVGA colour monitor, monochrome monitor, 270 MB H.D.D. and 8 MB RAM.

1.3.2 Software Details

The standard packages "ILWIS - 1.41" , "IDRISI", "GRAPHER" and "Microsoft Excel" have been used on the PC machine. ILWIS: the Integrated Land and Water Information System, version 1.41 is used for modelling, maximum likelihood classification, clustering, k-Nearest Neighbour and GIS purposes in the present study. ILWIS is a GIS that integrates image processing and spatial analysis capabilities, tabular databases and conventional GIS characteristics. All word processing work has been carried on MS Word version 6.0. Grapher and Microsoft Excel has been used for preparation of graphs.

1.4 Objectives and Scope

The broad objective of present study is to evaluate the potential of ANN classification and its best use in remote sensing applications. On application part the objective is to utilise remote sensing for delineating saline zones and to model the spectral behaviour of soil salinity taking into account both, ground field data and IRS-1B data. Various Scope of present study are as follows:

- to test the efficiency of ANN over their counter part in digital classification on identical test data.
- the effect of training set size and composition on ANN classification.
- studying and analysing the effect of moisture and salinity in soil and also developing a model to predict them using ground data and IRS-1B data.
- monitoring the change in aerial extent of salt affected regions in two seasons using satellite data..

1.5 Organisation of the Work

The present study is organised and presented in seven chapters. Chapter one deals with the brief introduction of the problem, data used, objective and scope of the work. Chapter two includes literature review. It mainly gives the comparative study of earlier works related with different unsupervised and supervised classification with special emphasis on neural network classifier. The general description of artificial neural network is in Chapter three.

Chapter four deals with details of conventional classification. A comparative study of conventional and ANN classifiers is presented in Chapter five.

Chapter six is related to spatial modelling and quantitative analysis of soil moisture and salinity parameters with ground and satellite data. An attempt is made to detect the soil salinity patches using artificial neural network is also presented in this chapter. Finally, the last Chapter seven is the summary of present work that relates with conclusion of whole work and future recommendations. The list of important Computer Programs developed and used for thesis are given in Appendix.

BACKGROUND OF WORK

Digital remotely sensed data contain wealth of information in which useful features can be identified and image may be classified using various parametric and non parametric procedures. Literature review has been carried out with the view to test the potential of different classifiers in case of remotely sensed images. The aim of present study is to investigate the most effective use of artificial neural network and its potential for classification and problem in implementation. Image classification procedures automatically categorize all pixels in an image into land cover classes or themes (Lillesand and Kiefer, 1994). For remote sensing purposes, normally the multispectral data available from the satellite is used, and the spectral pattern within the data for each pixel is used as the numerical basis for categorization. Digital number (DN) values depend on inherent spectral emittance and reflectance properties of Earth features which helps in their discrimination. Thus, a *spectral pattern* is not geometric in nature. The procedure that utilises pixel-by-pixel spectral information as the basis for automated land cover classification is called *Spectral Pattern Recognition* (Lillesand and Kiefer, 1994). The present literature review is mainly concentrated on Artificial Neural Network for image classification.

Artificial neural network models have been studied for many years in the hope of achieving human like performance in the field of image recognition. These models are composed of many nonlinear computational elements operating in parallel and arranged in patterns reminiscent of biological neural nets. Computational elements or nodes are connected via weights that are typically adapted during use to improve performance.

Work on artificial neural net models has a long history. Development of detailed mathematical models began more than 40 years ago with the work of McCulloch and Pitts, Hebb, Rosenblatt, Widron and others. More recent work by Hopfield, Rumelhart and McCelland, Sejnowski, Feldman, Grossberg and others has led to a new resurgence of the field. This new interest is due to the development of new net *topologies*, *algorithms* and new analog VLSI implementation techniques with some intriguing demonstrations as well as by a growing fascination with the functioning of the human brain. ANN may be divided into two groups: unsupervised and supervised classification types. They are discussed in following paragraphs.

2.1 Unsupervised Classification

Sometimes it can be useful to classify image without forcibly using any preconceived idea of how the pixels are grouped for different cover classes in feature space - this is the approach of *unsupervised classification.*

Kohonen's name is associated with two very different studies. Specifically, Kohonen initiated study of the prototype generation algorithm called Learning Vector Quantization (LVQ); and he also introduced the concept of Self-Organizing Feature Maps (SOFM) for visual display of certain one and two dimensional data sets. The detail of Kohonen algorithm is given in Chapter 3.

The self-organizing maps have a bearing on traditional vector quantization. Jari A. Kangas (1990) discussed the basic algorithms and two innovations: dynamic weighting of the input signals at each cell, which improves the ordering when very different input signals are used and definition of neighborhoods in the learning algorithm by the minimal spanning tree, which provides a far better and faster approximation to prominently structured density functions. Finally, it is cautioned that if the maps are used for pattern recognition and decision processes, it is necessary to fine tune the reference vectors so that they directly define the decision borders.

Okan K. Ersoy (1990) presented a new neural network architecture called the parallel, self-organizing, hierarchical neural network. The new architecture involves a number of stages in which each stage can be a particular neural network. At end of each stage, error detection is carried out, and a number of input vectors are rejected. Between two stages there is a nonlinear transformation of those input vectors rejected by the previous stage. The new architecture has many desirable properties such as optimized system complexity in the sense of minimized self-organizing number of stages, high classification accuracy, minimized learning and recall times, and truly parallel architectures in which all stages are operating simultaneously without waiting for data from each other operating simultaneously during testing. The experiments performed in comparison to multi-layered networks with back-propagation training indicated the superiority of the *new architecture.*

M. Schaale (1995) has presented land surface classification using neural networks. In this work spectral data from blue to near-infrared (IR) were sampled at three different dates in 1992 from a fire damaged forest region near Berlin (Germany) and have been analyzed principal component analysis, by the Normalized Difference Vegetation Index (NDVI) and by a Self-Organizing Feature Map (SOFM) algorithm. The properties of SOFM are summarized and it is shown that the introduction of lateral network connections allows an easy clustering of the resulting topological feature space. The SOFM reveals interesting land surface features and suggests, with the clustering scheme applied, further work with this new type of classification algorithm.

Yoshihisa Hara (1994) has done radar image classification using unsupervised classification, which determine classes automatically, but generally show limited ability to accurately divide terrain into natural classes. A new terrain classification technique is introduced to determine terrain classes in polarimetric SAR images, utilizing unsupervised neural networks to provide automatic classification, and employing an iterative algorithm to improve the performance. Several types of unsupervised neural networks are first applied for the classification of SAR images, and the results are compared to those of more conventional unsupervised methods. Results show that one neural networks method

Learning Vector Quantization (LVQ) outperforms the conventional unsupervised classifiers, but is still inferior to supervised methods. To overcome this poor accuracy, an iterative algorithm is proposed where the SAR image is reclassified using Maximum Likelihood Classifier (MLC). It is shown that this algorithm converges, and significantly improves classification accuracy. Performance after convergence is seen to be comparable to that obtained with MLC, while maintaining the advantages of an unsupervised techniques.

Andrea Baraldi (1995) presented implementation of an artificial neural network (ANN) which performs unsupervised detection of recognition categories from arbitrary sequences of multi-valued input patterns. The proposed ANN is called Simplified Adaptive Resonance Theory Neural Network (SARTNN). First, an Improved Adaptive Resonance Theory 1 (IART-1) based neural network for binary pattern analysis is discussed and a model is extended to multi-valued input pattern clustering and SARTNN is presented. A normalized coefficient which measures the degree of match between two multi-valued vectors, the Vector Degree of Match (VDM), provides SARTNN with the metric needed to perform clustering. Every ART architecture guarantees both plasticity and stability to the unsupervised learning stage. The SARTNN plasticity requirement is satisfied by implementing its attentions subsystem as a self-organized, feed-forward, flat Kohonen's ANN (KANN). The SARTNN stability requirement is properly driven its orienting subsystem. SARTNN processes multi-valued input vectors while featuring a simplified architectural and mathematical model with respect to both the ART-1 and the ART-2 models, the latter being the ART model fitted to multi-valued input pattern categorization. While the ART-2 model exploits ten user-defined parameters. SARTNN requires only two user-defined parameters to be run: the first parameter is the vigilance threshold, ρ. that affects the network's sensibility in detecting new output categories, whereas the second parameter, τ. is related to the network's learning rate. Both parameters have an intuitive physical meaning and allow the user to choose easily the proper discriminating power of the category extraction algorithm. The SARTNN performance is tested as a satellite image clustering algorithm. A chromatic component extractor is recommended in a satellite

image preprocessing extractor is recommended in a satellite image preprocessing stage, in order to pursue SARTNN invariant pattern recognition. In comparison with classical clustering algorithms like ISODATA, the implemented system gives good results in terms of ease of use, parameter robustness and computation time. SARTNN should improve the performance of a Constraint Satisfaction Neural Network (CSNN) for image segmentation. SARTNN, exploited as a self-organizing first layer, should also improve the performance of both the Counter Propagation Neural Network(CPNN) and the Reduced connectivity Coulomb Energy Neural Network (RCENN).

Tomoji Yoshida (1994) proposed a pattern classification method for remote sensing data using neural networks. First, he applied the error back-propagation (BP) algorithm to classify the remote sensing data. In this case, the classification performance depends on a training data set. In order to get stable and precise classification results, the training data set is selected based on geographical information and Kohonen's self-organizing feature map. From the classification results of the proposed method they showed that the present algorithm is more powerful than the conventional Bayesian method. Although the mean squares error of this method is not smaller than that of the BP method, the proposed method does not require perfect geographic information about training data set. Using the training data set and the error back-propagation algorithm, a layered neural network is trained such that the training patterns are classified with a specified accuracy. After training the neural network, some pixels are deleted from the original training data set if they are incorrectly classified and a new training data set is built up. Once training is complete, a testing data set is classified by using the trained neural network. Furthermore, from the confusion matrices they saw that the present method produces the best average and overall accuracies. As far as the future problem is concerned, it should be considered how to find the number of output layers by the Kohonen's method, the categories number, the neurons number at hidden layer by the BP algorithm. The classification results of LANDSAT TM data show that this approach produces excellent results which are more realistic and noiseless compared with a conventional method.

Yehuda Salu (1993) classified the multispectral image data by the binary diamond neural network and by nonparametric, pixel-by-pixel methods. The study deals with the application of nonparametric pixel-by-pixel classification methods in the classification of pixels, based on their multispectral data. A new neural network, the Binary Diamond, is introduced, and its performance is compared with a nearest algorithm and a back-propagation network. the Binary Diamond is a multilayer, feed-forward neural network, which learns from examples in unsupervised, "one-shot" mode. It recruits its neurons according to the actual training set, as it learns. The comparisons of the algorithms were done by using a realistic data base, consisting of approximately 90 000 Landsat 4 Thematic Mapper pixels. the Binary Diamond and the nearest neighbor performances were close, with some advantages to the Binary Diamond. The performance of the back-propagation network lagged behind. An efficient nearest neighbor algorithm, the binned nearest neighbor, is described. Ways for improving the performances, such as merging categories, and analyzing pixels, are addressed and evaluated.

2.2 Supervised Classification

Supervised classification follows the general model of pattern. There is an initial learning or training phase followed by the actual classification. In the training phase it is customary to identify pixels in test images for which ground data is available in order to localize specific ground cover classes in feature space. Once this phase has been undertaken a discriminator function must be devised to divide the feature space into regions for classification purposes. Researcher from many disciplines are interested in the use of remotely-sensed data to enhance their research. Standard classification methods usually require assumptions about the underlying statistics of the data, the most common being that the data for each ground cover class in Gossip distributed (e.g., Richards 1986, Schowengerdt 1983, Swain 1978). If these assumptions turn out to be correct then the statistical classifier is the optimal choice for the problem. In recent years the artificial neural network, or multi-layer perception, has been developed and applied to general pattern recognition problems. Neural network classifiers are non-parametric and may be

more robust when distributions are strongly non-Gaussian (Lippmann 1987). Because of this capability, researchers have begun investigating the use of this method for classifying remotely-sensed multi-spectral imagery.

There are two stages involved in using neural networks for multi-spectral image classification: the training stage and the classification stage. Training data is similar to that used in a statistical classifier. The network is trained, typically by the backpropagation algorithm, until some targeted minimal error is achieved between the desired and actual output values of the network. Once training is complete, the network is used as a feed-forward structure to produce a ground cover classification for the entire image. The analysis and literature survey is mainly organized into following topical sections:

1. Network input.
2. Network architecture.
3. Training algorithms.
4. Comparisons to conventional classifiers.

2.2.1 Network input

The most commonly used image data has been Landsat Thematic Mapper (TM) Blonda et al. (1994), Fierens et al. (1994), Paola and Schowengerdt (1994), Solaiman and Mouchot (1994), Yoshida and Omatu (1994), Civco (1991, 1993), Inoue et al. (1993), Kamata and Kawaguchi (1993), Kanellopoulos et al. (1993), Li et al. (1993), Bischof et al. (1992), Geaga el al. (1992), Geaga el al. (1992), Heermann and Khazenie (1992), Kiang (1992), Cromp (1991), Liu and Xiao (1991), Mulder and Spreeuwers (1991), Hepner et al. (1990), Ritter and Hepner (1990), McClellan et al. (1989). Other studies have involved SPOT (Tzeng et al. 1994, Dreyer 1993, Wilkinson et al. 1992, Kanellopoulos et al. 1991), Landsat MSS (Cromp 1991, Benediktsson et al. 1990a), simulated HIRIS (Benediktsson et al. 1990b), merged AVHRR and SMMR (key et al. 1990, key et al.

1989), SSMI (Rau and Lure 1993), and digitized aerial photography (medina and Vasquez 1991).

As with any classification routine, preprocessing, or feature extraction, can condense the data and help the neural network differentiate the classes. For example, principle components analysis is often used to reduce dimensionally in classification problems . Beyond the initial phase of data reduction, however, additional non-linear processing of the data before presenting it to the network can result in linearly separable classes that dramatically decrease training time over the non-linearly separable case (Pao, 1989). Dreyer (1993) calculated a number of textural features based on grey-level statistics. He found the use of these features increased the accuracy of a "field class, had no effect for 'urban' and 'water' classes and actually decreased the accuracy of a 'forest' class. Key et al. (1990) also used texture calculations such as second moment and entropy to produce a single texture measure for each class pixel in the classification such as second moment and entropy to produce a single texture measure for each pixel in the classification of land cover and cloud types in the Arctic, with classification results superior to those of spectral pixel values only. Civco (1991), in a land cover classification, presented the network with a single mean vector for each class of the training data. This resulted in a large reduction in the training set size but forced a statistical measure into the training process.

2.2.2 Network architecture

While the structure of the first and last layers of the neural network are controlled by external factors, the number of hidden layers and their size must be determined experimentally. Table : 2.1 shows the data encoding techniques and network structures used in the surveyed papers.

Generally for classification of multispectral imagery a three layer (single hidden layer) fully interconnected network is sufficient and is the most common implementation seen in the literature. In many of the surveyed papers trial and error method has been used to

determine the number of hidden layer nodes that results in the best classification. Benediktsson et al. (1990b), with 20 bands represented as binary inputs and a structure that consisted of 240 inputs, 15 hidden layer nodes, and 3 output nodes. In the other paper by Benediktsson et al. (1990a), they determined that their 56 input, 10 output network required 32 hidden layer nodes. Bischof et al. (1992), using 13 input nodes per band (91 total inputs) and 4 output nodes, determined 5 hidden layer nodes to be optimal after trial runs with from 2 to 15 nodes. The classification performance did not change much with the hidden layer nodes ranging from 3 to 15.

Benediktsson et al. (1990b) used a two layer network (which they called a conjugate-gradient linear classifier) in the classification of high dimensional (simulated HIRIS data. They found that the linear classifier produced classification results that were similar to that of the standard three layer network. In their other paper (1990a) they comment that the use of a four layer network did not improve classification accuracy over the three layer (6-15-1) and four (6-6-15-1) network topologies. Kanellopoulos et al. (1991) have used a four layer network with a 6-18-54-20 configuration. As a starting point for determining the number of hidden layer nodes they assumed that, for an N-dimensional feature space, the first hidden layer requires at least 2N nodes to define decision regions (also Pao, 1989).

2.2.3 Training algorithm

Once the input data, class representation, and overall network topology have been determined, the following must be selected: training data, the network parameters such as learning rate and momentum, and the criterion for training termination. The first of these, training data selection, is a problem common to all supervised training algorithms. Civco used one training sample for minimum distance, the mean vector, per class in one study (1991) and 10 samples per class in another (1993). Hepner et al. (1990) used what they

Table 2.1: Summary of the data encoding techniques and neural structures

Authors	Imagery	Input data encoding	Output data encoding	Network structure
Benediktsson *et. al.* (1990a)	MSS, elevation slope, aspect data	Gray coding	Temperature and binary coding	56-32-10 56-32-4
Benediktsson *et. al.* (1990b)	60 bands of Simulated HIRIS	Binary coding, 12 bits per band	3 outputs, one per class	240-15-3 480-15-3 720-20-3
Bischof *et. at.* (1992)	7 TM bands	Coarse coding requiring 13 inputs per band. Also with 5 by 5, 7 by 7 window in band 5	4 outputs, one per class	91-5-4 116-8-4 140-8-4
Civco (1993)	6 TM bands	Individual pixel values	15 outputs, one per class	6-15-15
Dreyer (1993)	3 SPOT bands texture calculations	Individual pixel values	9 outputs, one per class	3-13-12-9 6-8-8-9 42-7-7-9
Heermann, Khazenie (1992)	3 TM bands	Binary data, 8 bits per band	5 outputs, one per class	24-24-5
Hepner *et. al.* (1990)	4 TM bands	3 by 3 window of pixel values in each band	4 outputs, one per class	36-10-4
Kannellopoulos *et. al.* (1991)	2 date SPOT	Individual pixel values	20 outputs, one per class	6-18-54-20
Key *et. al.* (1990)	Merged AVHRR and SMMR	Individual pixel values	12 outputs, one per class	7-10-12
Li and Si (1992)	10 band airborne spectrometer	Individual pixel values. Input patterns are normalized first	3 outputs for 5 classes coding unspecified	10-7-3
Wilkinson *et. al.* (1992)	2 dates of 3 SPOT bands	Individual pixel values	7 outputs, one per class	3-15-7 6-21-7

termed a 'minimal training set' consisting of a 10 by 10 training site for each class. A few others used similar training set sizes (e.g., Liu and Xiao 1991, Benediktsson et al. 1990 b). The largest training set used consisted of 22000 patterns (Heermann and Khazenie 1992). However, it was found that the accuracy of classification was not much different for this large set than for a much smaller set of 4200 patterns. According to the authors, the selection of the training data is probably more important for accurate classification than the size of the training data. The greatest disadvantage of ANN is time. It takes more time in training as compared to MLC. The time taken by training network is reported by some researcher and given in Table 2.2.

Heermann and Khazenie (1992) devoted a section of their paper to the preparation of their training set. They refer to a 'picking and packing' technique. The 'picking' is accomplished by first employing an unsupervised clustering algorithm. Then small homogeneous regions are hand selected to represent the ground cover classes. Eliminating duplicate pixels within a class avoids redundant calculations, and eliminating duplicate training values between classes ensures that the network will not be given contradictory training information. However, if the class labels for the training data are reliable (e.g., through extensive ground truth data), it may not be advisable to eliminate duplicate samples in different classes, because this might reduce the ability of the network to detect mixed classes. For the backpropagation algorithm, learning rate and possibly momentum terms must be specified. As with the hidden layer size, there is no way of selecting these parameters except by experimentation. A true gradient descent is obtained only if infinitesimal steps are taken (Rumelhart et al. 1986). The most rapid learning occurs for the largest learning rate that does not lead to oscillation. The use of a momentum term allows the learning rate to be higher. Kanellopoulos et al. (1991), however, found that the best results were obtained when the momentum term was eliminated and the learning rate was normalized to be proportional to the number of network weights. Heermann and Khazenie (1992) employed a similar technique but did not eliminate the momentum terms. Their learning rate was set equal to $C_0 * \frac{1}{P} * \frac{1}{N}$, where N is the total number of nodes in

the network, P is the total number of training patterns, and C_0 is a constant that they determined experimentally to be 10.

Another problem in the training of a neural network arises from the initial assignment of random weights. Since this assignment is completely independent of the data, training time can be long and repeated training, with the same input data, can have different results. The number of training, with the same input data, can have different results. The number of training cycles required to achieve the same average error can vary considerably with different initial weight configurations. Li and Si (1992) have addressed these problems by using Kohonen's self-organizing algorithm (Pao,1989), which performs an unsupervised clustering procedure, to initialize the weights between the input layer and the hidden layer. The second set of weights (between the hidden and output layers) is randomized as before. This method resulted in a dramatic increase in training speed. To obtain a similar error rate, the standard procedure of completely random weights required over 1000 iterations while the self-organizing method required only 26 iterations.

2.2.4 Comparisons to conventional classifiers

In order to examine the feasibility of neural networks for multi-spectral image classification, it is useful to compare the method to conventional statistical classifiers. The consensus in the literature reviewed is that the two methods are similar in accuracy. Some researchers, however, found the standard methods better than the neural network method (e.g., Solaiman and Mouchot (1994), Civco (1991), Mulder and Spreeuwers (1991), Benediktsson et al. (1990b). Benediktsson et al. who found the MLC to have an accuracy of 87.56 percent compared to 64.89 percent for the three layer backpropagation network, , note however, that their use of simulated Gaussian-distributed data gives the maximum-likelihood method an unfair advantage. Likewise, Civco (1991), who used only the mean vectors of each class for training, states that this method does not exploit the inherent variability of the image data. The MLC used mean and covariance statistics, but the neural

network used only the means. In a subsequent study , Civco (1993) found that using multiple samples per class for the network training resulted in an accurate classification.

Most of the authors, however, found that the neural network technique produced similar or superior classifications to those of the standard methods (e.g., Blonda et al. 1993, Fierens et al. 1994, Paola and Schowengerdt 1994, Yoshida and Omatu 1994, Kanellopoulos et al. 1993, Li et al. 1993, Bischot et al. 1992, Heermann and Khazenie 1992, Kiang 1992, Liu and Xiao 1991, Medina and Vasquez 1991, Short 1991, Benediktsson et al. 1990a, Key et al. 1989, 1990) Bischof et al. (1992) found that the MLC and three layer backpropagation networks achieved similar results. When the network was supplied with a window of pixel data, however, its accuracy increased another 4 percent relative to the ground truth. Paola and Schowengerdt (1994), Kamata and Kawaguchi (1993), Hepner et al. (1990). and Ritter and Hepner (1990) also used a 3 by 3 window as input to the network and found it to be superior to the pixel-by-pixel MLC. The comparison of different classifier in terms of accuracy are given in Table 2.3

2.3 Summary of Classification Review

The research reviewed here has established that the ANN approach is feasible for the classification of remotely sensed multi spectral imagery. Similar performance to that of conventional classifiers, such as MLC, has been achieved. However, further work is necessary before neural networks become a practicable alternative to conventional classifiers. While the method is easy to implement in software, easily adapts to a variety of input data, and has shown a similar accuracy of classification as conventional classifiers, the slow and sometimes inconsistent learning phase, and the necessity for specifying obscure parameters such as learning rate, hidden layer size, and training convergence criterion make the approach less accessible to the casual user. The greatest disadvantage of the ANN is the length of training time. While this can be mitigated with unsupervised pre-processing techniques, it is probably the major reason why statistical methods will continue to be favoured for some time.

Table 2.2 :Summary of the times required to reach the error criterion for backpropagation training.

Authors	Computer	Backpropagation training time
Heermann, Khazenie (1992)	HP 9000-385	3 weeks 3 days with adaptive learning rate
Hepner et. al. (1990)	Vax 8600	3.1 CPU hours
Key et. al. (1990)	IBM PC/AT	23 minutes
Mulder and Spreeuwers (1991)	Sun workstation	10 hours
Paola and Schowengerdt (1994)	Sun SPARC station 10	3 hours
Wilkinson et. al. (1992)	Sun SPARC station 2	4 hours

2.4 Soil Salinity

There are enough literature available on soil salinity and moisture content but these works are mainly based on visual interpretation of imagery acquired in appropriate bands to characterize the salinity status of the soil. Reflectance of salt surface increases with increasing wavelength upto about 1 μm on many soil surfaces, but salt induces a relative higher reflectance in blue band by masking ferric oxides. Often, salts have a low reflectance in the near infra red and high in red band in dry season. The salts have a low reflectance in the middle and near infrared bands. This is due to presence of water and hygroscope characteristics of many salts, or to high moisture content of fresh salts (Mougenot et. al., 1993, Saha et. al., 1990). They also dealt with spectral properties of different salts consisting of chlorides and sulfates. They used spectra of pure salts acquired with a laboratory spectrophotometer measuring in visible to middle infrared and compared characteristic's absorption bands of salts as present on soil surface. The study concentrated on the presence of chlorides, carbonates, and sulfates. Praveen Dwivedi (1995) has studied the same study area for salinity. The trust was to evolve the tools of digital image processing for visual identification of salt effected regions and also to estimate concentration of salt quantitatively. He also observed the spectral behavior of

Table 2.3 : Summary of accuracy of deifferent algorithms

Authors	Algorithms	Accuracy		
Z. K. LIU et al. (1991)	Minimum distance to mean	50.9 %		
	MLC	71.6 %		
	BP	65.79 %		
Benediktsson et al. (1990 b)		87.56 %		
	BP	64.89 %		
P Gang (1996)	*Neural Network*			
	Overall	96.0 %		
	Average	92.1 %		
Yoshihisa Hara (1994)	*Unsupervised:*			
	Migrating means method (ISODATA)	81.8%		
	K-means method	54.2%		
	ART	33.3%		
	LVQ	81.9%		
	Feature Map	78.5%		
	Supervised:			
	Maximum Likelihood (ML)	74.1%		
	Multilayer perceptron	72.6%		
	ML method (4-look)	83.4%		
Jonatha Lee et al. (1990)		*ANN*	*K-Nearest Neighbor*	
	With 10 % Training Data	82.00 %	71.00 %	
	With 20 % Training Data	94.00 %	84.32 %	
Justin D. Paola et al. (1995)		*MLC*	*ANN*	
915 Pattern Set:	Train Site Accuracy	99.0%	94.8 %	
	Test Site Accuracy	89.5 %	89.8 %	
	Total Training and Classification Time	590 s	8962 s	
297 Pattern Set	Train Site Accuracy	99.0 %	95.6 %	
	Test Site Accuracy	75.5 %	81.3 %	
	Total Training and Classification Time	590 s	3769 s	
108 Pattern Set	Train Site Accuracy	100.0 %	98.1 %	
	Test Site Accuracy	60.6 %	72.8 %	
	Total Training and Classification Time	590 s	1625 s	
Tomoji Yoshida (1994)	Bayesian method	*MLC*	*BP*	*B-BP*
	Average accuracy	48.02%	49.62%	75.01%
	Overall accuracy	61.49%	61.79%	85.53%

soil salinity by MGTR and laboratory studies.

These data have been used for identification of salinity patches in present study. The details of methodology and results are presented in Chapter six.

CHAPTER 3

ARTIFICIAL NEURAL NETWORK IN IMAGE CLASSIFICATION

3.1 Introduction

Artificial Neural Networks (ANN) are computational models composed of many non-linear processing elements arranged in patterns similar to biological neuron networks. Human decision processes are often too complex to be expressed neatly using conventional logic. One such complexity is that human reasoning can be biased. A decision maker may give different degrees of importance to different factors. In a commonly accepted model of the brain, a given neuron receives electrochemical input signals from many neurons through synapses - some inhibitory, some excitatory - at its receiving branches or dendrites. If and when the net sum of the signals reaches a threshold, the neuron fires, transmitting a new signal through its axon, across the synapses to the dendrites of the many neurons it is in turn connected with. In the artificial system, "neurons", essentially tiny virtual processors, are usually implemented in software. Given an input, an artificial neuron uses some function to compute an output. As the output signal is propagated to other neurons, it is modified by "synaptic weights" or interneuron connection strengths. the weights determine the final output of the network, and can thus be adjusted to encode a decried functionality.

3.2 The Biological Prototype

Artificial neural networks are biologically inspired; that is, researchers are usually thinking about the organisation of the brain when considering network configurations and algorithms. Knowledge about the brain's overall operation is so limited that there is little to guide those who emulate it. Hence, network designers must go beyond current biological knowledge, seeking structures that perform useful functions. In many cases, this necessary shift discards biological plausibility; the brain becomes a metaphor; networks are produced that are organically infusible or require a highly improbable set of assumptions about brain anatomy and functioning.

The human nervous system, build of cells called neurons, is of staggering complexity. An estimated 10^{11} neurons participate in perhaps 10^{15} interconnections over transmission paths that may range for a meter or more. Each neuron shares many characteristics with the other cells in the body, but has unique capabilities to receive, process, and transmit electrochemical signals over the neural pathways that comprise the brain's communication system. Dendrites extend from the cell body to other neurons where they receive signals at a connection point called a synapse. On the receiving side of the synapse, these inputs are conducted to the cell body. There they are summed, some inputs tending to excite the cell, others tending to inhibit its firing. When the cumulative excitation in the cell body exceeds a threshold, the cell fires, sending a signal down the axon to other neurons. This basic functional outline has many complexities and exceptions; nevertheless, most artificial neural networks model only this simple characteristics.

Acc No. A 123313

3.3 Artificial Neural Network

Artificial Neural Networks (ANN) are information processing systems. Various fields in which ANN is being utilized . These are image mainly classification, pattern matching, pattern completion, noise removal, optimisation, control etc. In recent past it has found its use in image classification of remotely sensed images. In present study, it is an attempt to test the performance of ANN (supervised and unsupervised) classification on remotely sensed satellite data. The present chapter deals with the fundamental elements of a neural network, such as input and output patterns, processing element, connections, threshold operations, neural network topologies, learning algorithms and recall dynamics.

Neural Networks consist of processing elements and weighted connections. Each layer in a neural network consists of a collection of processing elements (PEs). Each PE in a ANN collects the values from all of its input connections, performs a predefined mathematical operation (typically a dot product followed by a PE function), and produces a single output value.

The foundations of neural networks consist of an understanding of the nomenclature and a firm comprehension of the rudimentary mathematical concepts used to describe and analyse neural network processing. In broad sense, neural networks consists of three elements:

1. *Topology* - how a neural network is organised into layers and how those layers are connected.
2. *Learning* - how information is stored in the network.
3. *Recall* - how the stored information is retrieved from the network.

3.4 Input and Output Patterns

3.4.1 Processing elements

The PE is the portion of the neural network where all the computing is performed. Each PE collects the information that has been sent down its abutting connections and produces a single output value. There are two important qualities that a PE must possess:

1. PEs require only local information. All the information necessary for a PE to produce an output value is present at the inputs and resides within the PE. No other information about other values in the network is required.
2. PEs produce only one output value. This single output value is propagated down the connections from the emitting PE to other receiving PEs, or it will serve as output from the network.

3.4.2 PE Functions

PE functions, also referred to as activation functions or squashing functions, map a PE's (possibly) infinite domain to a prespecified range. There are several PE functions but five are regularly employed by the majority of neural networks:

1. Linear PE function
2. Step PE function
3. Ramp PE function
4. Sigmoid PE function
5. Gaussian PE function

3.5 Cluster Analysis and Unsupervised Learning

The unsupervised approach attempts to identify spectrally homogeneous clusters of pixels within the image. It results in spectral groupings that may have an unclear meaning from the user's point of view. Having established these, the analyst then tries to associate an information class with each group. The unsupervised approach is often referred to as clustering and results in statistics that are for spectral, statistical clusters.

In unsupervised learning, no desired outputs are known to the system, but learning proceeds driven by the input data alone. A concrete example of unsupervised techniques is clustering in which a sample of input items are given and the goal is to divide them into a set of clusters in such a way that some relevant criterion, often related to inter-cluster and intra - cluster variances are minimised.

It has been found that in areas of complex terrain the unsupervised approach is preferable to the supervised one. In such conditions if the supervised approach is used, the user will have difficulty in selecting training sites because of the variability of spectral response within each class. Consequently, *a priori* ground data collection may be very time consuming. Also, the supervised approach is subjective in the sense that the analyst tries to classify information categories which are often composed of several spectral classes whereas spectrally distinguishable classes will be revealed by the unsupervised approach, and hence ground data collection requirements may be reduced.

Clustering is a fundamental function that precedes the ability to count, for it enables us to separate things into distinct and consistent groups. It involves the fundamental ability to

estimate central tendency, to summarise or agglomerate, to find average values, and get to the essence or origin of many specifics as a whole. The central mathematical concept in clustering is the computation of central tendency, or mean value. In a Euclidean space with a uniform Cartesian co-ordinate systems we can define the distance, D_{kj}, between the *k*th cluster centre vector X_k and the *j*th pattern or data vector X_j as:

$$D_{kj} = \sqrt{\sum_{i=1}^{NBnd} (X_{ik} - X_{ij})2}$$

where N_{Bnd} is the number of bands under consideration. This formulation of Euclidean distance assumes that the scales of all measurement dimensions are uniform and comparable. The assumptions of the method are that the Euclidean instances, D, separating the n-points in a p-dimensional space are proportional to the dissimilarities between the objects, and secondly no objects can belong simultaneously to two clusters.

3.5.1 Self Organising Feature Map (SOFM)

The Self Organising Feature Map (SOFM) is a unsupervised learning where no expected output is presented to the neural network. The network, by its self-organising properties, is able to infer relationships and learn more as more inputs are presented to it. One advantage to this scheme is that one can expect the system to change with changing conditions and inputs. The Kohonen SOFM is a neural network system developed by Teuvo Kohonen of Helsinki University of Technology and is often to classify inputs into different categories(1968).

In many applications, however, there is no supervisory output value - only inputs are provided and some form of clustering is desired. Loosely clustering means that we seek to grap the data into categories so that data samples "close" to one another are grouped in the same group. In 1968, kohonen proposed a noval approach to clustering and organisation for unsupervised learning, called the self-organising feature map, often appreciated SOFM. This technique uses a grid to impose an initial topological and define neighbourhoods.

3.5.1.1 Algorithm of SOFM

Let x be an input vector to the SOFM. The competitive phase of the learning algorithm employed in the SOFM determines a winning neural unit whereas the co-operative phase of the learning algorithm updates the weights of the winner and the neural units in its neighbourhood. The learning algorithm for the SOFM could be described as follows:

1. The distances between the input vector x and all the reference vectors (i.e. the weight vectors) are computed using a prespecified distance measure.
2. A neural unit for which the corresponding weight vector is at a minimum distance from the input vector is determined and designated as winner.
3. The weight vectors corresponding to the winner and the neural units in its topological neighbourhood are updated to align them towards the input vector.

Steps 1 and 2 comprise the competitive phase of the learning algorithm whereas step 3 comprises the operative phase. Step1 through 3 of the learning algorithm are carried out

for each input vector that is presented to the SOFM. The learning rate is defined to be the constant of proportionality, indicating the extent to which the weight vectors are adjusted or updated towards a given input vector. The learning rate (updating rate) and the size of neighbourhood are reduced as the learning progresses.

One of the important properties of the SOFM is that it represents a topology preserving mapping or a topographic mapping. The location of the winning units in 2-D mesh of neural units comprising the competitive layer conveys some information about the input vector. Winning units that are proximate in the competitive layer correspond to input vectors that are proximate in the input vector space. If x_1 and x_2 are two input vectors with corresponding winnings units at locations r_1 and r_2 in the competitive layer, then r_1 and r_2 get closer and eventually coincide as x_1 and x_2 are made more and more similar. Conversely, if $r_1 = r_2$ one could conclude that the corresponding input vectors x_1 and x_2 are similar. A topographic mapping thus preserves topological relations in the input space while at the same time performing a dimensionally reduction (i.e., projection) of the input space onto the 2-D mesh of neural units in the competitive layer. A topographic map entails a suitably defined topological neighbourhood around a winning neural unit in the competitive layer also a distance metric associated with the topological neighbourhood. Common choices for a topological neighbourhood are rectangular or hexagonal respectively.

3.5.1.2 Kohonen's Self Organising Feature Maps

1. Self-organising map is a result of a nonparametic regression process that is mainly used to represent high dimensional, nonlinearly related data items in an illustrative, often two-dimensional display.
2. In Kohonen's model there won't be any hidden layers.
3. Kohonen's model is an unsupervised classification and clustering.
4. While dealing with self-organising maps, one deals with models in which the ordering of the neurons, i.e., within a layer structure, plays an important role. One is concerned with the question of how the neurons should organise their connectivity in order to optimise the spatial distribution of their reposes within the layer.
5. Training time for this model is less when compared to backpropagation model.

3.6 ANN as a Classifier

Classification of multispectral remote sensing data may be considered as a mapping, F, from a multidimentional grey value space into a discrete vector space of feature classes given by

$$F:[a,b,c,d,\ldots]^{MXN} \rightarrow \{A,B,C,\ldots\}^{MXN}$$

where: a, b, c, d, . . are *grey values* of the pixel in *different spectral bands*; A, B, C are the *feature classes*, and MXN is the total number of pixels in the image, in any of the spectral bands.

Table 3.1 An algorithm to produce Self-Organising Feature Maps

Step1: Initialise Weights

Initialise weights from N inputs to the M output nodes to small random values. Set the initial radius of the neighbourhood.

Step 2: Present New Input

Step 3: Compute Distance to All Nodes

Compute distances d_j between the input and each output node j using

$$d_j = \sum_{i=0}^{N-1} (X_i(t) - w_{ij}(t))2$$

where $X_i(t)$ is the input to node i at time t and $w_{ij}(t)$ is the weight from input node i to output node j at time t.

Step 4: Select Output Node with Minimum Distance

Select node j* as that output node with minimum d_j.

Step5: Update Weights to Node j* and Neighbours

Weights are updated for node j* and all nodes in the neighbourhood defined by $Ne_{j*}(t)$. New weights are

$$w_{ij}(t+1) = w_{ij}(t) + \eta(t)(x_i(t) - w_{ij}(t))$$

For $j \in Ne_{j*}(t)$ $\quad 0 \leq i \leq N-1$

The term $\eta(t)$ is a gain term $(0 < \eta(t) < 1)$ that decreases in time.

Step 6: **Repeat by Going to Step 2**

Perceptrons are feed-forwards type networks normally developed under supervision as classifier or associative memory. A single-layer perceptron or two-layer associative network is the simplest of all perceptron-type networks. It consists of an input layer connected directly with a layer of output neuron. A multilayer perceptron model consists

of additional layers of neuron, termed hidden layers, between the inputs and outputs layer of neuron.

The mapping function for a classifier can be simulated using a multilayer perception trained through a set of training data. The number of input units in the perceptron model is equal to the number of spectral bands involved in the classification. The number of output units is fixed by the number of feature classes for which the model is trained. The rest of the networks topology, that is the number of hidden layers and the numbers of hidden neurones in various hidden layers, are selected judiciously considering the distribution of the feature classes. Once the topology of the model is decided, the model using a set of training data. A trained network is characterised by its topology, node characteristics or transfer function, connection weights, and internal thresholds. The trained network can be used directly for classification simply by feeding the input vectors at the inputs nodes and selecting the output node with the highest value.

3.7 Backpropagation Training Algorithm

Until recently, there were no effective algorithms for adjusting the interconnecting weight values to achieve minimal overall training error in multi-layer networks. The *generalised delta rule*, or *backpropagation*, presented in 1986 by Rumelhart et al. is now one of the most commonly used methods. The algorithm is given in Table 3.2. This is an iterative, gradient decent training procedure.

3.7.1 The Generalised Delta Rule

In a generalised deltas learning scheme, all weights and thresholds first are set to small random numbers. Normally, the *Sigmoid transfer function* is used to compute the output of a neuron (O_{pj}).

$$O_{pj} = \frac{1}{(1+e^{-(netpj-\theta j)})}$$

where

net_{pj}= the net input received by the neuron j

$= \sum w_{ij} x_i$

w_{ij} = connection strength for a connection from a neuron i to j

x_i = an input, or the output from the neuron i

θ= internal threshold associated with node j.

Starting with the output node the weights and thresholds are adjusted, layer-by-layer, working back towards the input layer. Using the Sigmoid transfer function to compute the output of a neuron, the equations for modification of weights at t *th* iteration is given by:

$$\Delta w_{ji}(t) = \eta \delta_{pj} O_{pi} + \alpha w_{ji}(t-1)$$

where

Δw_{ji} = change in weight for a connection from a hidden node i or an input to a node j

3.7.2 Equations

Output of *j*th hidden layer neuron:

$$O_j = f((\sum_i x_i W_1[i][j]) - \theta_j)$$

Ouput of *j*th output layer neuron:

$$z_j = f((\sum_{Opi} W_2[i][j])\ \tau_j)$$

Ith component of vector of output differences:

$$\text{desired value - computed value} = P_i - z_i$$

Ith component of output error at the output layer:

$$e_i = (P_i - z_i)$$

Ith component of output error at the hidden layer:

$$t_i = O_{pi}\ (1 - O_{pi})(\ \sum_j W_2[i][j] e_j)$$

Adjustment for weight between *j*th neuron in hidden layer and *j*th output neuron:

$$\Delta W_2[i][j] = \eta_0 O_{pi} e_j$$

Adjustment for weight between *i*th input neuron and *j*th neuron in hidden layer:

$$W_1[i][j] = \eta_h x_i t_j$$

Adjustment to the threshold value or bias for the *j*th output neuron:

$$\Delta\tau_j = \eta_h e_j$$

For use of momentum parameter α

$$\Delta W_2[i][j] = \eta_0 y_i e_j + \alpha \Delta W_2[i][j](t-1)$$

and

$$\Delta W_2[i][j] = \eta_0 x_i t_j + \alpha \Delta W_1[i][j](t-1)$$

3.7.3 Limitations of the Backpropagation Algorithm

While the backpropagation algorithm is one of the most extensively used learning algorithms to train multilayered neural networks, it has several serious limitations that make its application a difficult proposition. Some of these include:

1. *Convergence:* No theoretical proof exits that the backpropagation algorithm will converge to the global minimum or even to a local minimum of the error function. It is always possible that the solution will oscillate around the minima.
2. *Rate of convergence:* The number of iterations needed for training the network is very large for practical problems, so that the time taken for convergence may sometimes be as high as several hours or even days.
3. *Convergence to a local minimum:* Due to the use of the steepest descent method, once the solution reaches a local minimum, it is not possible to move out of it onto another minimum. Therefore it cannot be guaranteed that the weight set obtained after the network converges corresponds to the global minimum of the error function.

Table 3.2: The Back-Propagation Training Algorithm

The back-propagation training algorithm is an iterative gradient algorithm designed to minimise the mean square error between the actual output of a multilayer feed-forward perceptron and the desired output. It requires continuous differentiable non-linearity's. The following assigns a sigmoid logistic nonlinearity is used where the function $f(\alpha)$ is

$$f(\alpha) = 1/(1+e^{-(\alpha-\theta)})$$

step 1. Initialise Weights and Offsets

Set all weights and node offsets to small random values.

step 2. Present Input and Desired Outputs

Present a continuos valued input vectors x_0, x_1,.....x_{N-1} and specify the desired outputs d_0, d_1,.....d_{M-1}. If the net is used as a classifier then all desired outputs are typically set to zero except for that corresponding to the class the input is from. That desired output is 1. The input could be new on each trial or samples from a training set could be presented cyclically until weights stabilise.

step 3. Calculate Actual Outputs

Use the sigmoid nonlinearity from above and formulas to calculate outputs $y_0, y_1, \ldots y_{M-1}$.

step 4. Adapt Weights

Use a recursive algorithm starting at the output nodes and working back to the first hidden layer. Adjust weights by

$$w_{ij}(t+1) = w_{ij}(t) + \eta\delta_j x_i$$

In this equation $w_{ij}(t)$ is the weight from hidden node I or from an input to node j at time t, x_j is either the output of node I or is an input, η is again term, and δ_j is an error term for node j. If node j is an output node, then

$$\delta_j = y_j(1-y_j)(d_j-y_j)$$

Where d_j is the desired output of node j and y_j is the actual output.

If node j is an internal hidden node, then

$$\delta_j = x_j(1-x_j)\sum\delta_k w_{jk}$$

where k is over all nodes in the layers above node j. Internal node thresholds are adapted in a similar manner by assuming they are connection weights on links from auxiliary constant-valued inputs. Convergence is sometimes faster if a momentum term is added and weight changes are smoothed by

$$w_{ij}(t+1) = W_{ij}(t) + \eta\delta_j x_j + \alpha(w_{ij}(t) - w_{ij}(t-1))$$

where $0<\alpha<1$.

step 5. Repeat by going to step 2.

Table 3.3: Performance measures and parameters for different neural architectures

Training \ Architecture	Performance measure	Parameters
Backpropagation \ Multilayer perceptron	Convergence speed	Learning parameter η Momentum parameter α
ART 1	Number of classes	Vigilance parameter ρ
Kohonen	convergence and labelling error	Learning rate α

Table 3.4: Well-know learning algorithms.

Paradigm	Learning rule	Architecture	Learning algorithm	Task
Supervised	Error - correction	Single or multilayer perceptron	Perceptron learning algorithms Backpropagation Adaline and Madaline	Pattern classification Function approximation Prediction, Control
	Boltzmann	Recurrent	Boltzmann learning algorithm	Pattern classification
	Hebbian	Multilayer feed-forward	Linear discriminant analysis	Data analysis Pattern classification
	Competitive	Competitive	Learning vector quantization	Within-class categorization Datacompression
		ART network	ART Map	Pattern classification Within-class categorization
Unsupervised	Error-correction	Multilayer feedforward	Sammon's projection	Data Analysis
	Hebbian	Feed-forward or competitive	Pricipal component analysis	Data analysis
	Competitive	Competitive	Vector quantization	Categorization Data compression
		Kohonen's SOM	Kohonen's SOM	Categorization data analysis
		ART networks	ART1, ART2	Categorization
Hybrid	Error-correction and competitive	RBF network	RBF learning algorithm	Pattern classification Function approximation prediction, control

$$a_i^n N_n = \theta_i^{n+1} \qquad 1 <= n <= M-1$$

$$1 <= i <= N_{n+1} - 1$$

The operation of node i in layer (n+1) is characterised by the equation

$$x_i^{n+1} = f$$

STATISTICAL CLASSIFIERS

4.1 Unsupervised Classification

In present study, two conventional classifiers have been used for accuracy comparison with ANN. The conventional methods of classification mainly based on two approaches: *unsupervised* and *supervised*. The unsupervised approach attempts to identify spectrally homogeneous clusters of pixels within the image. Pixels belonging to a particular cluster are therefore spectrally similar. In this technique an image is segmented into unknown classes. It is for the user to label those classes afterwards based on ground truth data. There are several algorithms available in unsupervised classification. The unsupervised clustering algorithm used in present study is detailed below.

In unsupervised clustering, first pixel is assigned to the first cluster in the cluster list. For every new pixel the spectral distance to all clusters is calculated. If distance for this cluster is less than the threshold distance as specified by the user then the pixel is added it, otherwise a new cluster is generated. When a pixel is added to a cluster an average is calculated for the cluster position. This position is used to determine distances to individual pixels.

Every time a pixel is handled, a check is made as to whether the maximum number of clusters has been reached, if so, the merging process is initiated. During merging, clusters that are closest to each other are merged until the distance between the closest clusters is

below a threshold determined by minimum cluster distance. The smallest clusters are discarded, until the user specified number of clusters remain left. The clusters left out are those that would have been merged with another cluster if no distance threshold had been applied. The unsupervised clustering algorithm is presented mathematically in Table:4.1.

Table 4.1: Unsupervised Clustering algorithm

Given a set of unlabelled samples $\{x_1, \ldots . x_N\}$

Step 1: Choose K initial cluster centres $c_1(1), \ldots . . c_K(1)$. These could be arbitrary, but are usually defined by

$$c_i(1) = x_i \qquad 1 \leq i \leq K$$

Step 2: At the *k*th step, assign the sample x_l, $1 \leq l \leq N$ to cluster *j* if

$$\| x_l - c_j(k) \| < \| x_l - c_i(k) \|$$

for all $i \neq j$. (In the case of equality we assign x_i arbitrarily to i or j)

Step 3: Let $C_j(k)$ denote the *j*th cluster after Step 2. Determine new cluster centres by

$$c_j(k+1) = \frac{1}{N_j} \sum_{x \in C_j(k)} x$$

where N_j = number of samples in $C_j(k)$. Thus, the new cluster centre is the mean of the samples in the old cluster.

4.2 Supervised Classification

The first step for supervised samples is representative or prototype pixels from each of the desired sets of classes. Training samples for each class can be identified by site visits, existing maps, air photographs or even photointerpretation of an FCC of the image. These training data are to use for estimating the parameters of the particular classifier. Now the classifier, it is trained to classify every pixel in the image into one of the desired cover types. Generally, three algorithms are used for conventional supervised classification: *minimum-distance-to-means, parallelepiped,* and *Maximum Likelihood Classifier* (MLC). The minimum-distance-to-means strategy is mathematically simple and computationally efficient but is insensitive to different degrees of variance in the spectral response of training pixels. The parallelepiped classification strategy is also computationally simple and takes into account the variances in training classes but problems may arise from parallelepiped overlap due to correlation amongst classes. The MLC quantitatively evaluates both the variance and covariance of training class pixels and assumes a normal distribution for training classes. Of the three classifiers, the MLC has been most widely used and provides best result as reported by earlier workers and discussed in Chapter 2. MLC has been used for comparison with Backpropagation. MLC is present in ILWIS 1.41 and has been used for present study and works as follows:

MLC performs multispectral classification using class statistics obtained in the training data by program sample. It calculates the statistics from maximum of 4 bands. The bands used in the training data correspond to the bands used for classification. The flow chart of MLC is presented in Fig. 4.2 (Dikshit, O., 1992) and detail about MLC classifier is given in Richard's (1986).

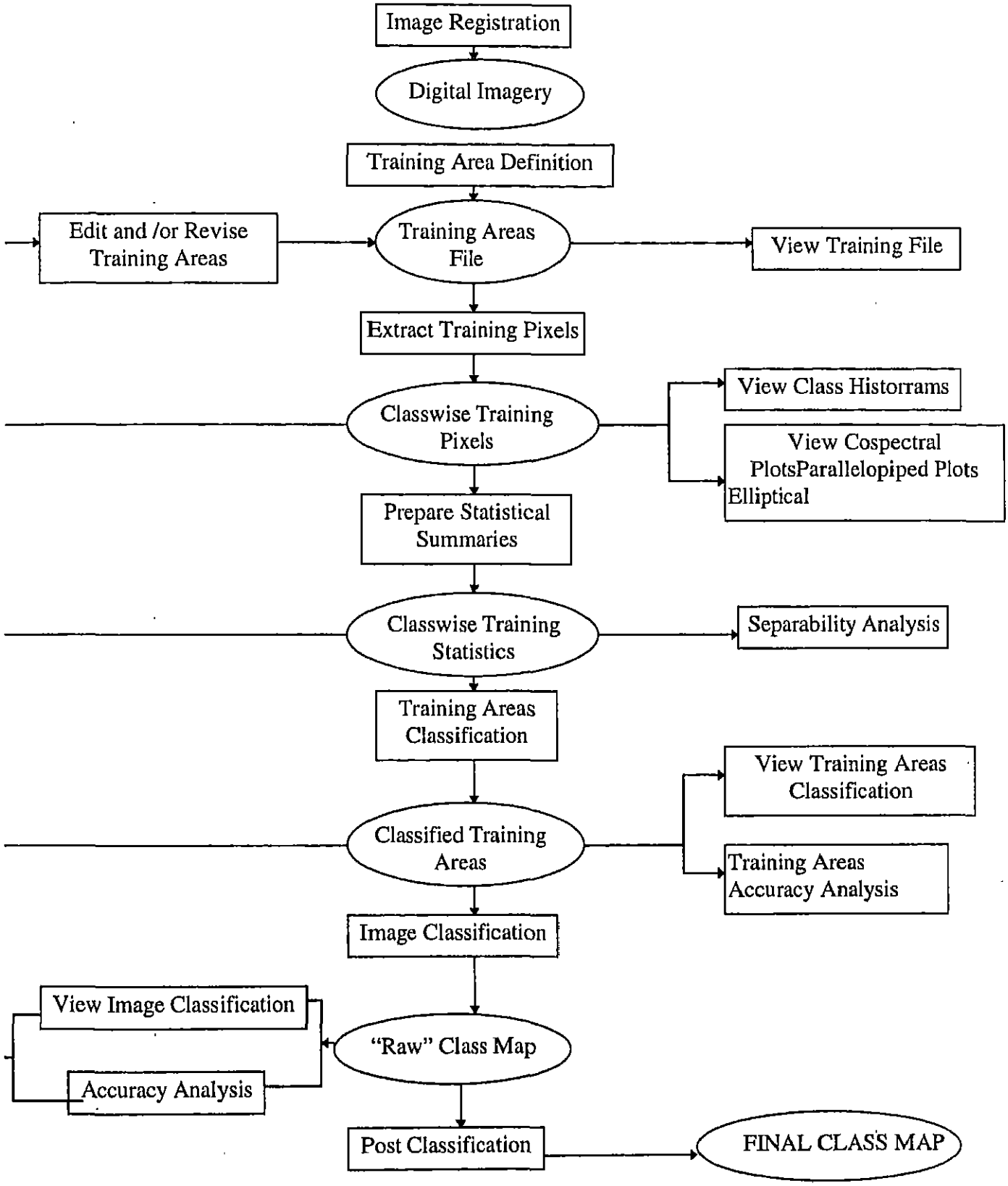

Figure 4.1: Supervised Approach of Classification using the Maximum Likelihood Classifier

CONVENTIOAL AND NEURAL CLASSIFIERS: A COMPARISON

5.1 General

In present study, two different ANN algorithms and two conventional classification algorithms have been investigated. The conventional classifiers used in present study are unsupervised clustering and Maximum Likelihood Classifier (supervised). ANN classifier tested in present study are unsupervised Self-Organising Feature Maps (Kohonen's algorithm) and supervised Backpropagation Learning. Potentials of backpropagation are evaluated at different front mainly at training data set. The performance of all classification has been assessed on the basis of the classification accuracy on the same test dataset. Objective of this investigation help in identifying the suitable classifier and may be subsequently used for salinity assessment.

5.2 Unsupervised Classification

The unsupervised approach is aimed at identify spectrally homogeneous sets of pixels within the image. Once spectral sets are identified, the analyst then tries to associate an information class with each group. The unsupervised approach is often referred to as *clustering*.

In unsupervised learning, no desired outputs are known to the system, but learning proceed is made driven by the input data alone. A concrete example of unsupervised technique is clustering in which a sample of input items is given and the goal is to divide them into a set of clusters in such a way that some relevant criterion, often related to inter-cluster and intra cluster variance is minimised. Self-Organising Feature Maps (SOFM)

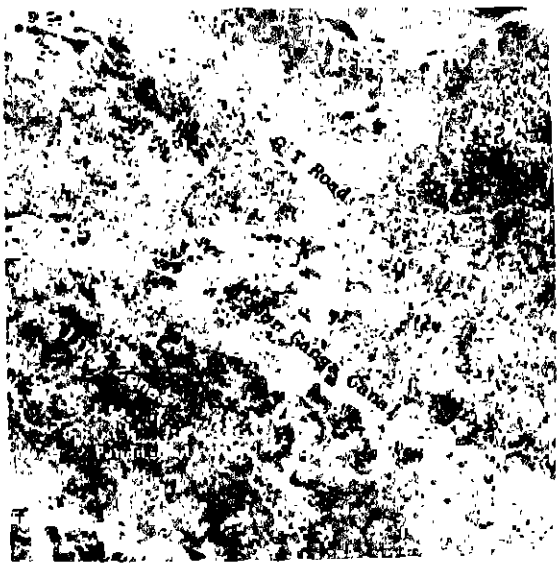

Figure 5.1: FCC of study area

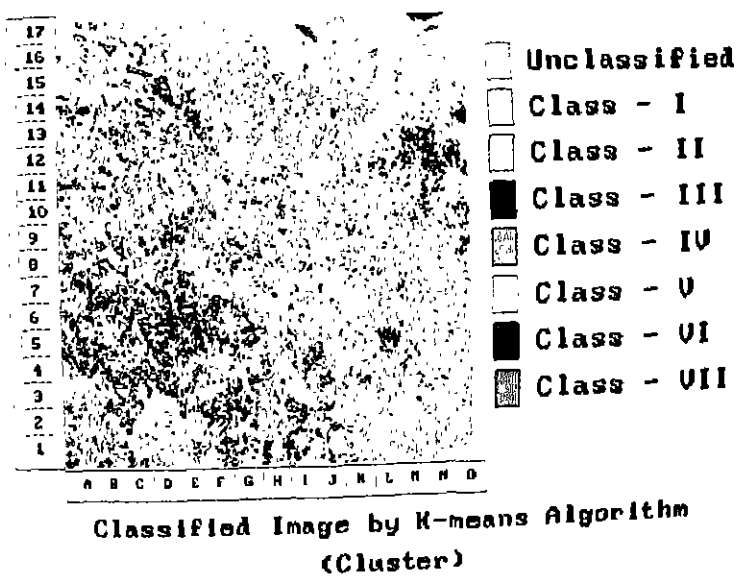

Figure 5.2 : Classified image by unsupervised clustering

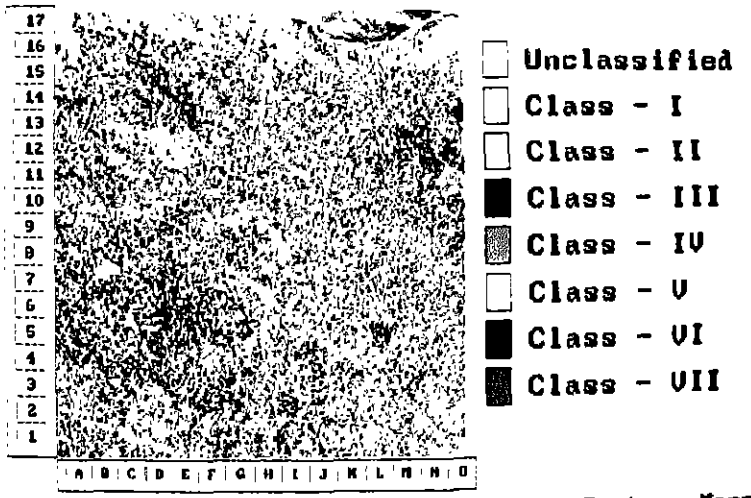

Figure 5.3: Classified Image by SOFM

classifies the input image data and forms clusters. For SOFM, band 3 data has been used. Pixel by pixel, input is presented to the network, without specifying the desired output. The weights are randomised using *random number generator* in C programming language. As required by the algorithm, this value is extremely small. To make this value the initial weight user interactive the multiplication factor is added. Hence, it is made comparable to the input data approach, and the multiplication factor is named as the orientation factor. The initial weight should be from 0.1 to 0.9 range. A rectangular topology has been used in present study. The initial radius 'n' has been selected for defining the neighbourhood for output of images and it shrinks with time. The radius is user interactive parameter. The value of radius should be larger than the desired number of output cluster. The number of output nodes, n, is taken as six in present study. The gain term is selected initially as 0.1 and it decreases with time. An accurate time function is not important: $\alpha = \alpha(t)$ can be linear, exponential, or inversely proportion to t. The $\alpha(t)$ expressed in eq. 5.1 may be reasonable choice for remote sensing images (Kohonen, T., 1995) and used in present study.

$$\alpha(t) = 0.9\ (1\text{-}t/100). \qquad (5.1)$$

In this approach different numbers of cluster were tried and finally seven classes were decided to check by both the algorithms. The same test image has been used for evaluating the performance in terms of accuracy. The accuracy for each class and confusion matrix has been obtained from program **r_format** and **c_confu**.

There are seven clusters in the classified image as shown in Fig.5.2 and 5.3. These classes have been matched with map, FCC (as shown in Fig. 5.1) and ground data. The comparison is made with existing information of study area. Class-I has been identified as crop. The confusion matrixes are presented in Table 5.1 and 5.2 respectively. The accuracy of each class has been compared in Table 5.3. It is evident from the result that SOFM performed better for this class. Class - II has been identified as Open Scrub Land. It is well distributed in the image but predominant in G-17, H-16, M-16, N-16. Class - III is saline soil and classified as salinity -II in supervised learning. It is having medium salinity level and classified well by both classifiers. Class - IV is *unclassified* by both the classifiers but SOFM totally failed to identify this class. The areas near D-12, D-13, E-12, and E-13 are unclassified pixels in SOFM but it is saline soil with high level of salinity. The accuracy of this class is very low. Classification using unsupervised clustering has yielded better result than SOFM in this class. Class - V is water body and delineated better in unsupervised clustering than SOFM as it is evident from the result. Class - VI is very poorly classified by both classifiers but SOFM again fail to identify this class. Class - VII is again a well-distributed class in whole area and identified as mixed urban. The graphical representation of accuracy of each class is given in Fig. 5.4. Quantitative comparison of unsupervised clustering versus SOFM indicates that SOFM has performed better for three classes (I, II and III). It was not found able to discriminate the classes IV and VI. The unsupervised clustering performed better for four classes (IV, V, VI and VII). The overall accuracy of SOFM is 67.6 as compared to 73.1 in unsupervised clustering. The two classes are mainly unclassified by SOFM. The overall performance of SOFM is better for best five classes as shown in Table 5.4. The area of each of the classified classes has been calculated as reported in Table 5.5.

Table 5.1: Confusion Matrix for unsupervised clustering for test image

Classes	Pixels	Classified as							
		1	2	3	4	5	6	7	unclassified
1	503	391	3	6	23	0	34	21	25
2	1198	0	646	0	139	0	11	0	402
3	747	0	12	633	17	0	43	11	31
4	769	0	37	13	352	0	2	0	365
5	498	0	0	0	0	487	0	0	11
6	498	0	7	3	13	2	308	53	112
7	695	0	2	0	6	16	3	627	41
Total	4908	391	707	655	550	505	399	712	987

Table 5.2: Confusion Matrix for SOFM for test image

Classes	Pixels	Classified as							
		1	2	3	4	5	6	7	unclassified
1	503	465	11	2	0	3	0	0	22
2	1198	11	845	0	201	13	0	2	126
3	747	3	28	677	7	9	0	2	21
4	769	24	0	11	195	23	0	4	512
5	498	0	0	0	0	413	0	0	95
6	498	0	0	3	0	0	161	0	335
7	695	0	0	23	7	19	0	550	96
Total	4908	503	884	716	410	480	161	558	1207

Table 5.3: Comaprison of accuracy

	Test Data	
Classes	Unsupervised Clustering (%)	SOFM (%)
1	77.7	92.5
2	53.9	70.5
3	84.7	90.6
4	45.8	25.3
5	97.8	82.9
6	61.8	32.4
7	90.2	79.2
Total	73.1	67.6

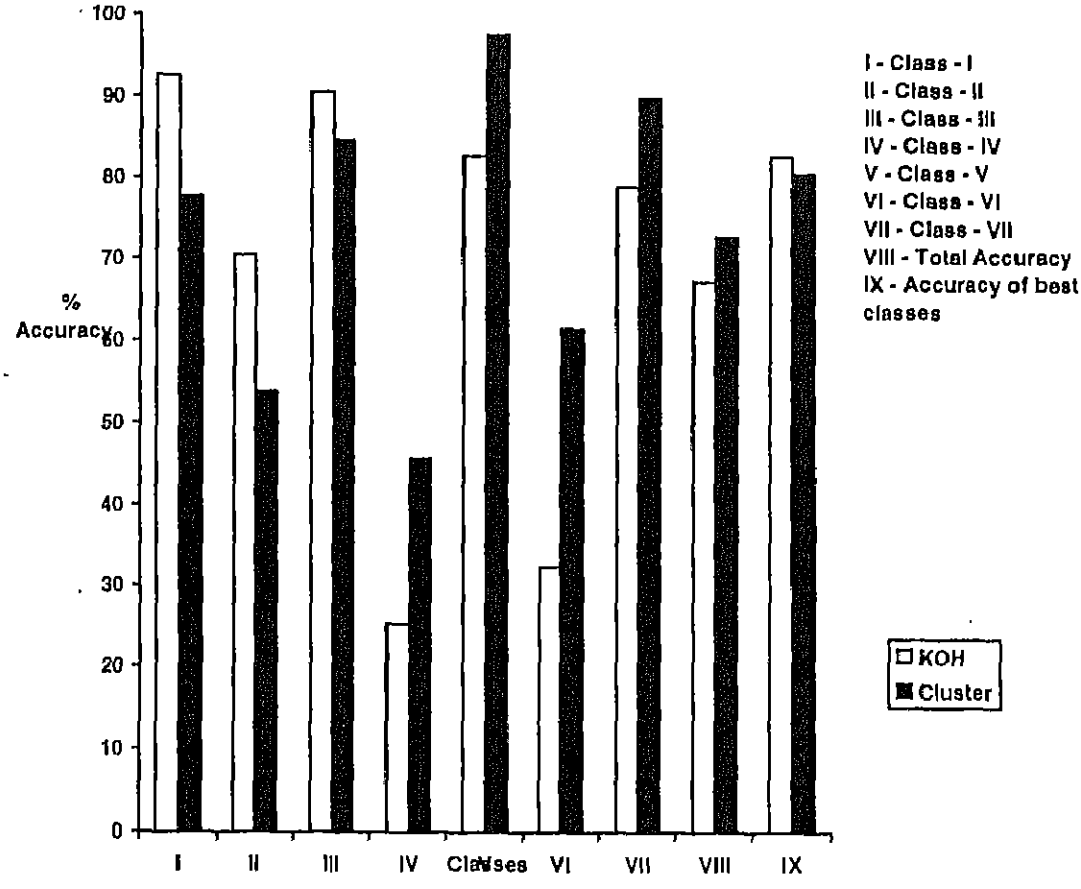

Figure 5.4: Comparison of accuracy of different classes and total by unsupervised classifier

Table 5.4: Comparison of accuracy of best five classes

	Test Data	
Classes	Cluster (%)	Koh (%)
1	77.7	92.5
2	53.9	70.5
3	84.7	90.6
5	97.8	82.9
7	90.2	79.2
Total	80.9	83.1

Table 5.5: Area of different classes in classified images

Classes	Area (ha)	
	Unsupervised Clustering	SOFM
Class - I	1440.33	3240.74
Class - II	7291.67	7921.81
Class - III	6811.56	6511.49
Class - IV	690.16	108.02
Class - V	207.05	360.08
Class - VI	1043.48	2167.36
Class - VII	7730.42	7947.79
Unclassified	3450.79	3090.71
Total	30006.87	30006.87

5.3 Supervised Classification

Seven classes have been identified by ground survey, published map of the study area and classification after unsupervised learning. These classes are

1 - Water

2 - Open Scrub Land

3 - Salinity - I

4 - Salinity - II

5 - Crop

6 - Mixed Urban

7 - Vegetation

To determine relative performance with training inputs, 200 pixels were specified for each of seven classes. Main water bodies of study area are mainly river Ganga, river Pandu, Lower and Upper Ganga canal. A large portion of land is in Open Scrub Land. Farmers of this area are facing acute problem of salinity. It is mainly due to over irrigation of the land through dense network of canal. Two discrete zones of this area are taken as classes. The other class is crop that varies with season and details are studied using spatial modelling in Chapter 6. Mixed Urban class consists of roads, building, build up areas and other

available urban features. Seventh class is chosen as dense vegetation, which consists of forest, orchards and different species of trees.

A flow chart of the steps involved in the classification of multispectral digital remote-sensing data using an ANN model as shown in Fig. 5.5. False Color Composites (FCC) of the digital images are used for training sites of various feature classes which are based on ground truth data. For simplicity of software implementation, only rectangular training sites are considered. The rectangular training sites are specified in terms of the co-ordinates of the top left-hand and bottom right-hand corner of the training sites. Feature classes are encoded as integer numbers starting with zero. All these informations are stored in GT file. Program **trn_sig_ext.c** uses this GT file to extract the training data set from the input images. The input vectors of classes with lower representation in the training data set are repeated so that each class has an equal representation. The input vectors are also rearranged so that the input vector for each feature class occurs at a regular interval. This provides a faster rate of learning.

5.3.1 Algorithm and software

Program **ann_trainer.c** uses this reshuffled training data set to train the multilayer perceptron model. Various model parameters, for example number of input units, output units, hidden layers and hidden neurons in various layers, the learning factors etc., are selected interactively during the execution of the program. For each input vector, the error is computed at the output nodes and the network parameters, that is weights and internal thresholds, are adjusted in accordance with the generalised delta rule. The network is trained repeatedly until the number of cycles of training reaches a predefined limit or the r.m.s. error at the output nodes for a complete cycle falls below a predefined threshold.

A test classification of the training data set to assess the performance of the classifier is done through the program **con_mat_gen.c**. A confusion matrix is generated by this program that can be used to evaluate the performance of the classifier. This confusion matrix compares the classified data with the actual training data through a resubstitution of training pixels in the network.

The actual classification of the images is done by the program **ann_classifier.c** using the trained binary network file. The grey value for a feature class in the classified image is the

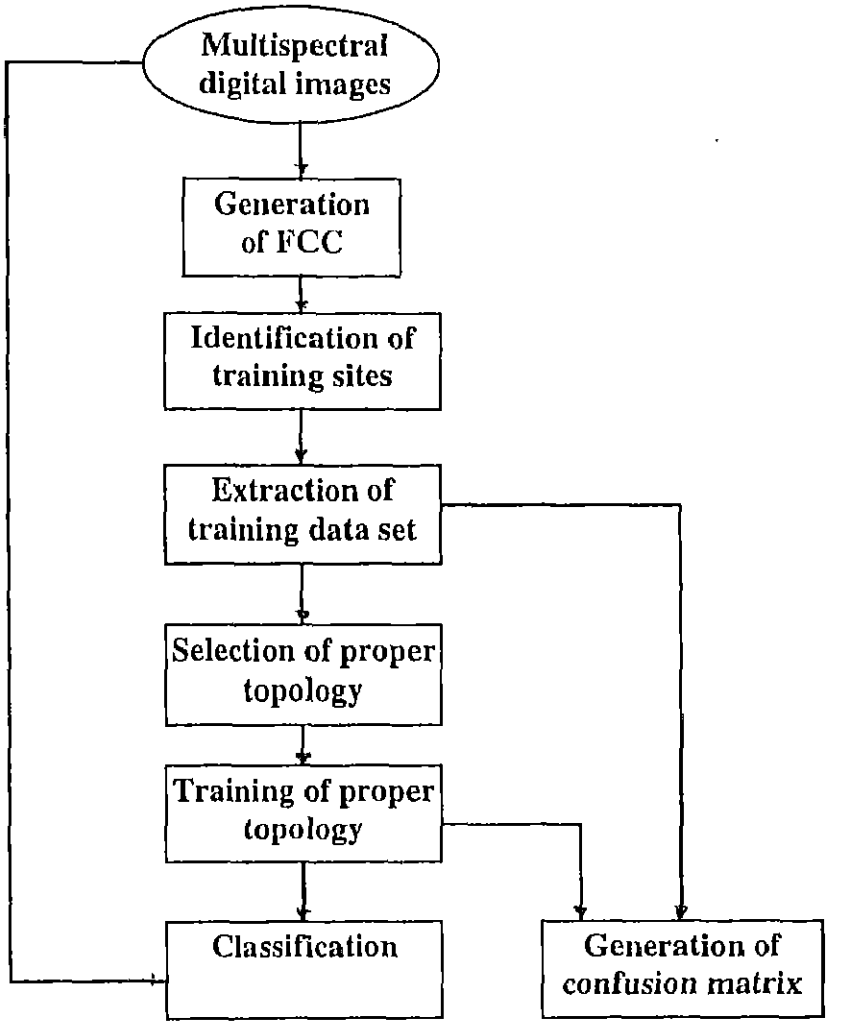

Figure 5.5: A flow chart Backpropagation Learning

same as the feature code used for the class. Results of the classification are given in terms of numbers of pixels and geographical coverage of all feature classes in addition to the classified image. Functions that are common to more than one program also are supplied.

Classification of the test data is to check the accuracy of classified image. This is done by using program **r_format** and **c_confu**. The confusion matrixes of classification are presented from Table 5.13 to 5.16 and percentage accuracy is in Table 5.17.

5.3.2 Configuring the network

In present work, the standard backpropagation training routine, with an adaptive learning rate and momentum, have been used. The particular adaptive algorithm has been defined heuristically and adopted based on encouraging results obtained by earlier workers as discussed in Chapter 2. The original idea was to keep the learning rate at a level just below the point at which it causes instability. This leads to faster, yet stable, training. After a user-defined number of training cycles, the mean square error is compared with that of the previous cycle. If the error has increased, the learning rate and momentum are halved. If the error has decreased, the learning rate and momentum are increased by 20%. This allows for accelerated convergence when the error is steadily decreasing.

For input to the network, the grey level values have been scaled within zero to one. For the training stage of supervised pattern recognition, the network weights are adjusted in an iterative, and gradient decent training procedure called backpropagation. The training data consist of a pair of data vectors. The input data vector is the desired set of output values to be produced by the network upon recall of that training pattern. The goal of the training is to minimize the overall error between the desired and actual outputs of the network. In order to guarantee the decrease in error, the incremental adjustments in the weights at each iteration must be infinitesimal. In order to achieve a realistic training time, a *leaning rate* parameter, which represents the percentage of the step taken towards minimum error must be specified. If this quantity is too small, training will take too long, and if it is too large, the gradient decent will degenerate and the error will increase. The *momentum parameter*, like the learning rate, is set at the beginning of the training and must be determined experimentally. The ANN classifier training has been conducted for different rate, momentum parameter and error. Study reveals that 1000 iterations are optimum to produce the desire results with above mentioned parameters. The number of iteration can be changed and it depends upon above mentioned parameters.

With these values sets, the remaining parameters are the number of hidden layers and number of nodes per hidden layer. It was assumed that a 3 - layer neural network (one hidden layer) would be sufficient for this type of classification and would provide similar discrimination abilities as the MLC (Paola, 1995). Thus, the sole parameter to be considered was the number of nodes in the single hidden layer. If we view both the neural networks and MLC as decision making functions defined by a number of parameters (degrees of freedom), then it is logical to use the same number of parameters in each for comparison. For a three layer network, assuming one input node per image band and one output node per class, the number of parameters as a function of network structure is

$$N_{net} = 3 + Wn$$

$$= 3 + Hn*(Nb + Nc) \qquad (5.2)$$

Where,

Wn = Total no. of weights

Hn = No. of hidden layer nodes

Nb = No. of bands

Nc = No. of classes

Where the first constant term is the number of parameters needed to specify the size of each of the three layers.

For the maximum - likelihood classifier, the corresponding number of parameters is

$$N_{ML} = 2 + Nb*Nc + 0.5*Nc(Nb^2 + Nb) \qquad (5.3)$$

The number of parameters is quadratic for the MLC with respect to the number of bands, while the number of parameters for the neural network method will depend on the choice of hidden layer size, which is not necessarily dependent on the number of bands.

Setting N_{NET} equal to N_{ML} and solving for the number of hidden layer nodes, we obtain

$$Hn = \frac{(2 + Nc * Nb + 0.5 * Nc * (Nb^2 + Nb) - 3)}{(Nb + Nc)} \qquad 5.4$$

From this calculation no. of hidden layer nodes is coming out to 9 for 7 classes and 4 bands. The training network used for present study is shown in Fig. 5.6.

5.4 Training Set

Training set characteristics have a significant effect on the performance of classification. The ground (training) data to be used in relation to the mapping technique which may to some extent be considered independent of the remotely sensed data, in Typically land cover is mapped from a remotely sensed image through use of a supervised image classification. A range of techniques has been used but conventional statistical classifiers such as the MSc are the most widely used (Matter 1987, Thomas et. al. 1987). Unfortunately, this type of classification makes a number of often untenable assumptions about the data set to be classified. In order to satisfy these assumptions and use the classifier correctly a large ground data set is required. It has, for instance been recommended that to form a representative training sample, the size of the training set for each class in the classification be at least 30 times the number of discriminating variables (e. g., wavebands) in the analysis (Swain 1978, Mather 1987). Combined with the other assumptions, the classifier makes about the data set (e.g., normally distributed data) apparently an appropriate ground data set is rarely available or used in conventional image classifications. Although the effect and significance of these issues may vary between data sets and may not always be a problem, alternative classification schemes will sometimes be required specially when spatial resolution is increasing and lot of mixed pixels are coming in the image to get a large number of training set. One possible alternative is to use an

artificial neural network. This comprises a set of simple interconnected units that work in parallel to categorise input data into output classes and such networks may classify data more accurately than conventional statistical classifiers. It has been reported that artificial neural networks may be used with minimal training sets but there is little information available on the effect of training set

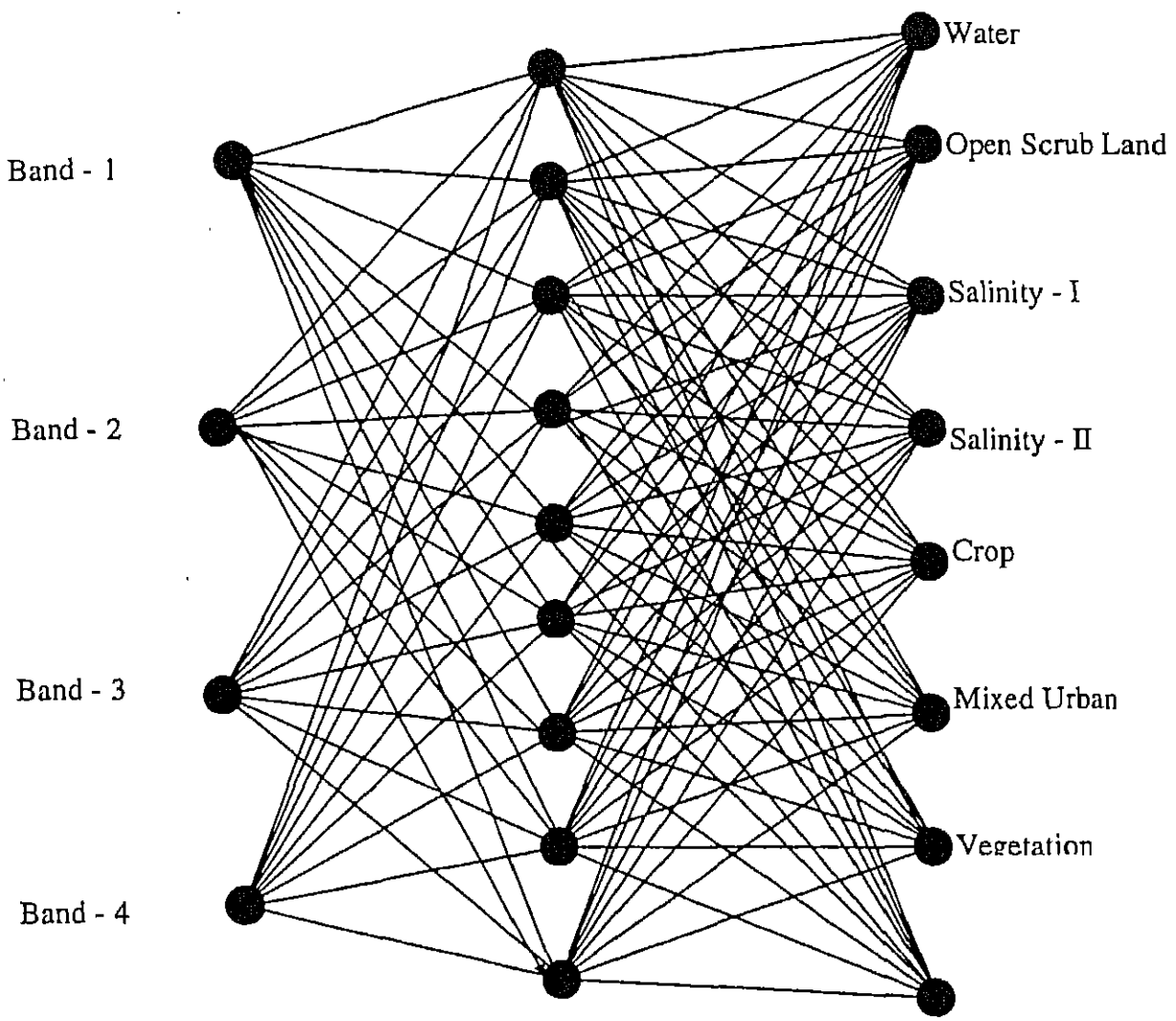

Figure 5.6 : ANN network for present study

size, in terms of the number of training samples, and other characteristics on classification performance. The aim of present part of study is to investigate the effects of variations in

training set size and composition of an artificial neural network, and the results will be evaluated against a MLC. for comparative purposes.

5.4.1 Training samples

Training sets of different size were derived by sampling for each class. The total training set size varied but each training set contained an equally sized sample for each class. Six of these training set were formed with the number of training cases for each class being a sample of 25, 50, 75, 100, 150 and 200 for training.

Two classification techniques used in the analysis were MLC and the Backpropagation Learning Algorithm (BPL) (program developed in 'c' by the author). Classifications of both the training data and testing data sets were performed. The classification of the training data set provides an indication of inter-class separability and illustrates how well the classifier 'learns' the training data. The accuracy of the training classification is, however, likely to over-estimate the true level of inter-class separability and attention should therefore focus mainly on the accuracy of the classification of the independent testing set. The accuracy of each classification was assessed from a confusion matrix and expressed as the percentage correct allocation and presented from Table 5.6 to 5.10. The relative performance of each of classifier has been evaluated by comparing classification accuracies and the pattern of class allocation, displayed in the confusion matrix.

5.5 Result and Discussion

To assess the effect of variation is overall training set size, the present remote sensing image was classified by both the MLC and the BPL algorithm using the series of training sets that contained equal number of cases of training for each class but different in overall size. The Accuracy with which both the training and testing set were classified was assessed for each classification and the results are summarised in Fig. 5.7 which show that both classifiers are showing very high accuracy from 93.7 to 99.4 percent in training classification but MLC results are better in case of training, which is not true reflection of

overall accuracy of the image. To evaluate the performance of overall accuracy of the image, the test dataset has been made and tested by each classifier. The accuracy varies from 49.4 to 89.76 percent for different set of training data in case of MLC as presented in Table 5.10c. In case of BPL, the accuracy of test data varies from 67.4 to 91.32 percent and its results are supplied in Table 5.10d for different set of training set size. Furthermore, the relative differences in the classification accuracies, derived from the MLC and backpropagation, were larger with the smaller training set sizes. This was particularly noticeable for the training classifications, which may indicate over learning of the training patterns with consequent reduction in generalisation capacity; although the network has been constructed and run in a manner designed to avoid over learning. Nevertheless, results show that BPL provided a higher degree of inter-class separability than MLC, specially in case of a small training set. The test accuracies for 25 training pixels are 49.4 and 67.4 for MLC and BPL respectively. The largest differences in accuracy were apparent in the classification of the training data, specially when overall training set size was small. ANN are more appropriate for classification when the training set is limited in size, and the generally more accurate than conventional statistical classifier.

Same 200 pixels of each class were taken for training BPL and MLC. These sites were carefully selected to be homogeneous and free of extraneous cover types. The mean and standard deviation of training sample used are in Table 5.11 and 5.12 respectively.

The output image produced by MLC using the same training data is shown in Fig 5.9. The river Ganga may be seen from I-17 to O-17 of curved shape. River Pandu is from A - 9 to O - 1 but these features are more distinct in classified image by ANN presented in Fig. 5.10. The accuracy of water is 91.6 and 98.6 percent in case of MLC and ANN respectively. Open Scrub Land area is clearly identified by both the classifier and its concentration,from I - 16, I - 17 to N - 16, O - 17 is marked. Salinity has been classified fairly well by both the classifiers. Crop is also very well distributed class but it is classified better as 93 percent in case of ANN. Vegetation is classified well by ANN and mainly located near C-13, D - 13, E - 12 and E - 13. The overall classification accuracy is 91.32

percent in case of ANN and 89.76 percent in case of MLC. The detail comparison of each class is presented in Table 5.17. The overall quality of the ANN classification is shown by the relatively homogeneous regions, sharp transition boundaries and continuous connected features, which are characteristically speckled / noisy on MLC. Preliminary results indicate that the ANN can classify imagery better than a statistical classifier procedure using identical training sites. Results of supervised classification using the single minimal training site have been found to be inferior to the ANN classification. These results suggest that the ANN offers a more robust approach to land cover discrimination than the vastly used MLC. One of the major problems associated with recognition and classification of patterns from remotely sensed data is the time and cost of developing a set of training sites and training the ANN classifier. The graphical presentation of accuracy of each of classes is in Fig 5.11 and area belongs to each class is in Table 5.18. The comparison between the classified image of BPL and MLC has been made and found that only 73.74 percent area is common in both the images as shown in Table 5.19.

Code for different classes:
1- Water, 2 - Open Scrub Land, 3 - Salinity - I, 4 - Salinity - II, 5 - Crop, 6 - Mixed Urban, 7 - Vegetation.

5.6 Training Accuracy for Backpropagation Classifier

Table 5.6a : ***Confusion Matrix*** for Bacpropagation classification of training image for 25 pixels in training for each class.

Classes	Pixels	Classified as							
		1	2	3	4	5	6	7	unclassified
1	25	23	0	0	0	0	0	0	2
2	25	0	25	0	0	0	0	0	0
3	25	0	0	25	0	0	0	0	0
4	25	0	0	0	25	0	0	0	0
5	25	0	0	0	0	25	0	0	0
6	25	0	0	0	0	0	24	0	1
7	25	0	0	0	0	0	0	25	0
Total	175	23	25	25	25	25	24	25	3

Table 5.6b : ***Confusion Matrix*** for Bacpropagation classification of training image for 50 pixels in training for each class.

Classes	Pixels	Classified as							
		1	2	3	4	5	6	7	unclassified
1	50	48	0	0	0	0	0	0	2
2	50	0	49	0	0	0	0	0	1
3	50	0	0	48	0	0	0	0	2
4	50	0	1	1	47	0	0	0	1
5	50	0	0	0	0	49	0	0	1
6	50	0	0	0	0	0	47	0	3
7	50	0	0	0	0	0	0	49	1
Total	350	48	50	49	47	49	47	49	11

Table 5.6c : ***Confusion Matrix*** for Bacpropagation classification of training image for 75 pixels in training for each class

Classes	Pixels	Classified as							
		1	2	3	4	5	6	7	unclassified
1	75	69	0	0	0	0	0	0	6
2	75	0	75	0	0	0	0	0	0
3	75	0	0	73	0	0	0	0	2
4	75	0	1	0	72	0	0	0	2
5	75	0	0	0	0	73	0	0	2
6	75	0	0	0	0	0	69	0	6
7	75	0	0	0	0	0	0	71	4
Total	525	69	76	73	72	73	69	71	22

Table 5.6 d : ***Confusion Matrix*** for Bacpropagation classification of training image for 100 pixels in training for each class

Classes	Pixels	Classified as							
		1	2	3	4	5	6	7	unclassified
1	100	95	0	0	0	0	0	0	5
2	100	0	95	0	0	0	0	0	5
3	100	0	0	93	2	0	0	0	5
4	100	0	0	2	91	0	0	0	7
5	100	0	0	0	0	96	0	0	4
6	100	0	0	0	0	0	94	0	6
7	100	0	0	0	0	0	0	94	6
Total	700	95	95	95	93	96	94	94	37

Table 5.6e : ***Confusion Matrix*** for Bacpropagation classification of training image for 150 pixels in training for each class

Classes	Pixels	Classified as							
		1	2	3	4	5	6	7	unclassified
1	150	142	0	0	0	0	0	0	8
2	150	0	144	0	1	2	0	0	3
3	150	0	0	139	6	0	0	0	5
4	150	0	0	4	142	0	0	0	4
5	150	0	3	0	0	141	0	1	5
6	150	0	0	0	0	0	136	0	14
7	150	0	0	0	0	0	0	140	10
Total	1050	142	147	143	149	143	136	141	49

Table 5.6f : ***Confusion Matrix*** for Bacpropagation classification of training image for 200 pixels in training for each class

Classes	Pixels	Classified as							
		1	2	3	4	5	6	7	unclassified
1	200	188	0	0	0	0	0	0	12
2	200	0	186	0	1	4	0	0	9
3	200	0	0	186	3	0	0	0	11
4	200	0	0	3	191	0	0	0	6
5	200	0	2	0	0	188	0	0	10
6	200	0	0	0	0	0	183	0	17
7	200	0	0	0	0	0	0	193	7
Total	1400	188	188	189	195	192	183	193	72

5.7 Training Accuracy for Maximum Likelihood Classifier

Table 5.7a : ***Confusion Matrix*** of Maximum Likelihood Classifier of training image for 25 pixels in training for each class.

Classes	Pixels	Classified as							
		1	2	3	4	5	6	7	unclassified
1	25	24	0	0	0	0	0	0	1
2	25	0	25	0	0	0	0	0	0
3	25	0	0	25	0	0	0	0	0
4	25	0	0	0	25	0	0	0	0
5	25	0	0	0	0	25	0	0	0
6	25	0	0	0	0	0	24	0	1
7	25	0	0	0	0	0	0	25	0
Total	175	24	25	25	25	25	24	25	2

Table 5.7b : ***Confusion Matrix*** of Maximum Likelihood Classifier of training image for 50 pixels in training for each class.

Classes	Pixels	Classified as							
		1	2	3	4	5	6	7	unclassified
1	50	49	0	0	0	0	0	0	1
2	50	0	49	0	0	0	0	0	1
3	50	0	0	48	0	0	0	0	2
4	50	0	0	1	49	0	0	0	0
5	50	0	0	0	0	49	0	0	1
6	50	0	0	0	0	0	50	0	0
7	50	0	0	0	0	0	0	50	0
Total	350	49	49	49	49	49	50	49	5

Table 5.7c : ***Confusion Matrix*** of Maximum Likelihood Classifier of training image for 75 pixels in training for each class.

Classes	Pixels	Classified as							
		1	2	3	4	5	6	7	unclassified
1	75	73	0	0	0	0	0	0	2
2	75	0	75	0	0	0	0	0	0
3	75	0	0	73	0	0	0	0	2
4	75	0	1	0	72	0	0	0	2
5	75	0	0	0	0	73	0	0	2
6	75	0	0	0	0	0	72	0	3
7	75	0	0	0	0	0	0	74	1
Total	525	73	76	73	72	73	72	74	12

Table 5.7d: ***Confusion Matrix*** of Maximum Likelihood Classifier of training image for 100 pixels in training for each class.

Classes	Pixels	Classified as							
		1	2	3	4	5	6	7	unclassified
1	100	99	0	0	0	0	0	0	1
2	100	0	99	0	0	0	0	0	1
3	100	0	0	93	2	0	0	0	5
4	100	0	0	2	97	0	0	0	1
5	100	0	0	0	0	96	0	0	4
6	100	0	0	0	0	3	97	0	0
7	100	0	0	0	0	0	0	96	4
Total	700	99	99	95	99	99	97	96	16

Table 5.7e : ***Confusion Matrix*** of Maximum Likelihood Classifier of training image for 150 pixels in training for each class.

Classes	Pixels	Classified as							
		1	2	3	4	5	6	7	unclassified
1	150	142	0	0	0	0	0	0	8
2	150	0	144	0	1	2	0	0	3
3	150	0	0	147	3	0	0	0	0
4	150	0	0	2	148	0	0	0	0
5	150	0	3	0	0	141	0	1	5
6	150	0	0	0	0	0	144	0	6
7	150	0	0	0	0	0	0	140	10
Total	1050	142	147	149	152	143	144	141	32

Table 5.7e : ***Confusion Matrix*** of Maximum Likelihood Classifier of training image for 200 pixels in training for each class..

Classes	Pixels	Classified as							
		1	2	3	4	5	6	7	unclassified
1	200	198	0	0	0	0	0	0	2
2	200	0	197	0	1	2	0	0	0
3	200	0	0	193	0	0	0	0	7
4	200	0	2	6	192	0	0	0	0
5	200	0	0	0	0	194	0	0	6
6	200	0	0	0	0	0	193	0	7
7	200	0	4	3	0	0	0	189	4
Total	1400	198	203	202	193	196	193	189	26

5.8 Test Accuracy for MLC

Table 5.8a : ***Confusion Matrix*** of Maximum Likelihood Classifier of test image for 25 pixels in training for each class.

Classes	Pixels	Classified as							
		1	2	3	4	5	6	7	unclassified
1	498	238	0	0	0	0	0	0	260
2	1198	0	707	0	7	0	0	0	484
3	769	0	0	519	11	0	0	0	239
4	747	0	10	0	408	0	0	0	329
5	503	0	0	0	0	207	0	0	296
6	695	0	0	0	0	0	165	0	530
7	498	0	0	0	0	0	0	259	239
Total	4908	238	717	519	426	207	165	259	2377

Table 5.8b : ***Confusion Matrix*** of Maximum Likelihood Classifier of test image for 50 pixels in training for each class

Classes	Pixels	Classified as							
		1	2	3	4	5	6	7	unclassified
1	498	301	0	0	0	0	0	0	197
2	1198	0	841	0	8	0	0	0	349
3	769	0	0	542	3	0	0	0	224
4	747	0	20	136	373	0	0	0	218
5	503	0	0	0	0	220	0	0	283
6	695	0	0	0	0	0	487	0	208
7	498	0	0	0	0	0	0	358	140
Total	4908	301	861	678	384	220	487	358	1619

Table 5.8c : ***Confusion Matrix*** of Maximum Likelihood Classifier of test image for 75 pixels in training for each class

Classes	Pixels	Classified as							
		1	2	3	4	5	6	7	unclassified
1	498	303	0	0	0	0	0	0	195
2	1198	0	860	0	22	2	0	0	314
3	769	0	0	457	18	0	0	0	294
4	747	0	24	25	504	0	0	0	194
5	503	0	0	0	0	426	0	1	76
6	695	0	0	0	0	0	566	0	129
7	498	0	0	0	0	0	0	424	74
Total	4908	303	884	482	544	428	566	425	1276

Table 5.8d : ***Confusion Matrix*** of Maximum Likelihood Classifier of test image for 100 pixels in training for each class

Classes	Pixels	Classified as							
		1	2	3	4	5	6	7	unclassified
1	498	399	0	0	0	0	0	0	99
2	1198	0	927	0	83	2	0	0	261
3	769	0	0	612	2	0	0	0	155
4	747	0	7	143	476	0	0	0	251
5	503	0	23	0	0	417	0	0	63
6	695	0	0	0	0	0	603	0	92
7	498	0	0	0	0	0	0	354	144
Total	4908	399	957	755	561	419	603	354	1065

Table 5.8e : ***Confusion Matrix*** of Maximum Likelihood Classifier of test image for 150 pixels in training for each class

Classes	Pixels	Classified as							
		1	2	3	4	5	6	7	unclassified
1	498	436	0	0	0	0	0	0	62
2	1198	0	1037	0	32	28	0	2	99
3	769	0	0	608	10	0	0	0	151
4	747	0	7	121	560	0	0	0	59
5	503	0	9	0	0	480	0	2	12
6	695	0	0	0	0	0	634	0	61
7	498	0	0	0	0	0	0	438	60
Total	4908	436	1037	602	602	508	634	442	504

Table 5.8f : ***Confusion Matrix*** of Maximum Likelihood Classifier of test image for 200 pixels in training for each class

Classes	Pixels	Classified as							
		1	2	3	4	5	6	7	unclassified
1	498	456	0	0	0	0	0	0	42
2	1198	0	1040	0	39	43	0	1	75
3	769	0	0	698	13	0	0	0	58
4	747	0	41	24	657	0	0	2	23
5	503	0	3	0	0	457	0	1	42
6	695	0	0	0	0	13	636	0	46
7	498	0	0	0	14	11	0	442	31
Total	4908	456	1084	722	723	524	636	445	317

5.9 Test Accuracy for ANN

Table 5.9a : ***Confusion Matrix*** of Backpropagation of test image for 25 pixels in training for each class.

Classes	Pixels	Classified as							
		1	2	3	4	5	6	7	unclassified
1	498	257	0	2	0	0	0	0	239
2	1198	0	833	0	9	0	1	0	355
3	769	0	14	548	0	11	0	0	196
4	747	0	0	53	619	0	0	0	75
5	503	0	3	0	21	383	0	0	96
6	695	0	0	15	0	1	394	0	285
7	498	0	0	21	0	0	0	318	159
Total	4908	257	500	639	649	395	395	318	1355

Table 5.9b : ***Confusion Matrix*** of Backpropagation of test image for 50 pixels in training for each class

Classes	Pixels	Classified as							
		1	2	3	4	5	6	7	unclassified
1	498	387	0	12	0	0	0	0	77.7
2	1198	2	881	0	19	0	0	0	73.5
3	769	0	39	589	3	0	0	0	76.6
4	747	0	0	4	608	0	21	0	81.4
5	503	0	0	0	3	413	6	3	82.1
6	695	0	0	0	0	0	494	0	71.1
7	498	0	11	0	0	0	0	418	83.9
Total	4908	389	531	605	633	413	521	421	78.0

Table 5.9c : ***Confusion Matrix*** of Backpropagation of test image for 75 pixels in training for each class.

Classes	Pixels	Classified as							
		1	2	3	4	5	6	7	unclassified
1	498	413	0	7	0	0	0	0	78
2	1198	0	893	0	22	2	0	0	281
3	769	0	0	617	28	0	0	0	124
4	747	0	29	35	638	0	0	0	45
5	503	0	2	0	11	456	0	0	34
6	695	13	0	0	0	9	586	0	87
7	498	0	11	0	0	0	0	448	39
Total	4908	426	935	659	699	467	586	448	688

Table 5.9d : ***Confusion Matrix*** of Backpropagation of test image for 100 pixels in training for each class.

Classes	Pixels	Classified as							
		1	2	3	4	5	6	7	unclassified
1	498	429	0	3	0	0	0	0	66
2	1198	0	1013	13	3	0	0	0	149
3	769	0	0	663	2	0	8	0	96
4	747	0	0	43	676	0	0	0	28
5	503	11	0	0	11	452	0	0	29
6	695	0	0	0	0	0	604	0	91
7	498	0	0	0	0	0	0	458	40
Total	4908	440	1013	722	692	452	612	458	499

Table 5.9e : ***Confusion Matrix*** of Backpropagation of test image for 150 pixels in training for each class.

Classes	Pixels	Classified as							
		1	2	3	4	5	6	7	unclassified
1	498	434	0	5	0	0	0	0	59
2	1198	0	1018	0	149	4	0	0	27
3	769	0	0	713	37	0	0	0	19
4	747	0	13	4	618	0	0	0	112
5	503	0	0	0	0	434	0	13	56
6	695	3	0	0	0	0	593	0	3
7	498	0	0	0	0	11	0	468	29
Total	4908	437	1031	722	804	449	593	481	305

Table 5.9f : ***Confusion Matrix*** of Backpropagation of test image for 200 pixels in training for each class.

Classes	Pixels	Classified as							
		1	2	3	4	5	6	7	unclassified
1	498	493	0	0	0	0	5	0	0
2	1198	0	1021	39	33	0	0	0	105
3	769	0	0	684	19	0	0	0	66
4	747	0	5	0	668	4	0	0	70
5	503	0	0	2	17	468	0	1	15
6	695	0	0	0	14	3	626	1	51
7	498	0	21	0	4	0	0	467	6
Total	4908	493	1047	725	755	475	631	469	313

5.10 Comparison of Different Classes

Table: 5.10a: Percentage accuracy of training image for different set of sample by Backpropagation

	Percentage accuracy for different set of samples					
Classes	25 Pixels	50 Pixels	75 Pixels	100 Pixels	150 Pixels	200 Pixels
1	92.0	96.0	92.0	95.0	94.7	94.0
2	100.0	98.0	100.0	95.0	96.0	93.0
3	100.0	96.0	97.3	93.0	92.7	93.0
4	100.0	94.0	96.0	91.0	94.7	95.5
5	100.0	98.0	97.3	96.0	94.0	94.0
6	96.0	94.0	92.0	94.0	90.7	91.5
7	100.0	98.0	94.7	94.0	93.3	96.5
Total	98.3	96.3	95.6	94.0	93.7	93.9

Table: 5.10b: Percentage accuracy of training image for different set of training sample by Maximum Likelihood classifier

	Percentage accuracy for different set of samples					
Classes	25 Pixels	50 Pixels	75 Pixels	100 Pixels	150 Pixels	200 Pixels
1	96.0	98.0	97.3	99.0	94.7	99.0
2	100.0	98.0	100.0	99.0	96.0	98.5
3	100.0	96.0	97.3	93.0	98.0	96.5
4	100.0	98.0	96.0	97.0	98.7	96.0
5	100.0	98.0	97.3	96.0	94.0	97.0
6	100.0	100.0	96.0	97.0	96.0	96.5
7	100.0	100.0	98.7	98.0	93.3	89.5
Total	99.4	98.3	97.5	97.0	95.8	96.14

Table 5.10c: Percentage accuracy of test image for different set of training sample by Maximum Likelihood classifier

	Percentage accuracy for different set of samples					
Classes	25 Pixels	50 Pixels	75 Pixels	100 Pixels	150 Pixels	200 Pixels
1	47.8	60.4	60.8	80.1	87.6	91.6
2	59.0	70.2	71.8	77.4	86.6	86.8
3	67.5	70.5	59.4	79.6	79.1	90.8
4	54.6	49.9	67.5	63.7	74.9	87.9
5	41.2	43.7	84.7	82.9	95.4	90.9
6	23.7	70.1	81.4	86.8	91.2	91.5
7	52.0	71.9	85.1	71.1	87.9	88.8
Total	49.4	62.9	72.9	77.37	86.1	89.76

Table 5.10d: Percentage accuracy of test image for different set of training sample by Backpropagation

	Percentage accuracy for different set of samples					
Classes	25 Pixels	50 Pixels	75 Pixels	100 Pixels	150 Pixels	200 Pixels
1	51.6	77.7	82.9	86.1	87.1	98.9
2	69.5	73.5	74.5	84.6	85.0	85.2
3	71.3	76.6	80.2	82.2	92.7	88.9
4	82.9	81.4	85.4	90.5	82.7	89.4
5	76.1	82.1	90.1	89.9	86.3	93.0
6	56.7	71.1	84.3	86.9	85.3	90.1
7	63.9	83.9	89.6	92.0	94.0	93.8
Total	67.4	78.0	83.9	87.5	87.6	91.32

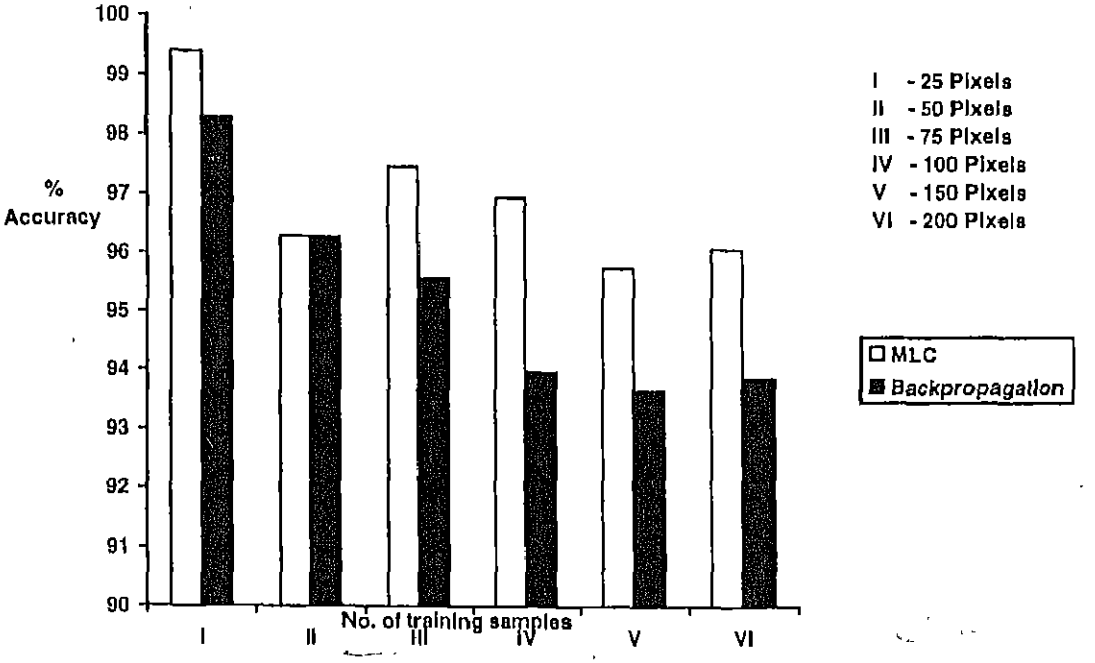

Figure. 5.7: Comparison of accuracy for different set of training samples of trining image

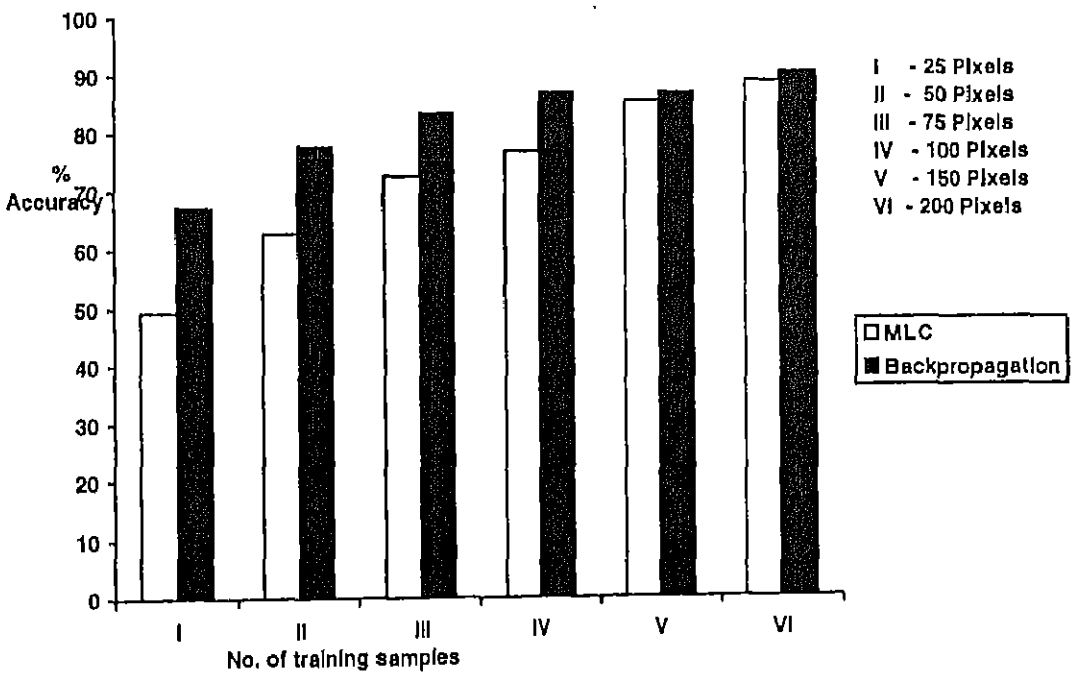

Figure 5.8: Comparison of accuracy for different set of sample set of test image

Table 5.11: Mean for training set data

Classes	Band - 1	Band - 2	Band - 3	Band - 4
River	56.4	33.3	40.9	27.7
Open Scrub Land	78.8	52.6	76.7	70.8
Salinity - I	103.7	70.8	102.2	90.2
Salinity - II	91.8	62.0	88.9	79.7
Crop	78.1	49.4	70.0	65.8
Mixed Urban	58.5	35.5	51.1	57.3
Vegetation	69.2	43.5	58.8	73.2

Table 5.12 Standard Deviations for training set data

Classes	Band - 1	Band - 2	Band - 3	Band - 4
River	2.8	2.4	2.5	2.8
Open Scrub Land	2.3	2.1	2.7	1.8
Salinity - I	2.8	2.4	2.9	2.9
Salinity - II	2.9	2.1	3.0	2.0
Crop	2.0	1.8	2.3	2.0
Mixed Urban	2.1	1.6	2.9	2.7
Vegetation	2.5	1.8	3.0	2.6

5.11 Comparison of Supervised Classifier

Code for different classes:
1- Water, 2 - Open Scrub Land, 3 - Salinity - I, 4 - Salinity - II, 5 - Crop, 6 - Mixed Urban, 7 - Vegetation.

Table 5.13: Confusion matrix for classification by Backpropagation algorithm for training data

		Classified as							
Classes	Pixels	1	2	3	4	5	6	7	unclassified
1	200	188	0	0	0	0	0	0	12
2	200	0	186	0	1	4	0	0	9
3	200	0	0	186	3	0	0	0	11
4	200	0	0	3	191	0	0	0	6
5	200	0	2	0	0	188	0	0	10
6	200	0	0	0	0	0	183	0	17
7	200	0	0	0	0	0	0	193	7
Total	1400	188	188	189	195	188	187	193	72

Table 5.14: Confusion matrix for classification by Maximum Likelihood classifier for training data

Classes	Pixels	Classified as							
		1	2	3	4	5	6	7	unclassified
1	200	198	0	0	0	0	0	0	0
2	200	0	197	0	1	2	0	0	0
3	200	0	0	193	0	0	0	0	7
4	200	0	2	6	192	0	0	0	0
5	200	0	0	0	0	194	0	0	6
6	200	0	0	0	0	0	193	0	7
7	200	0	4	3	0	0	0	189	4
Total	1400	198	203	202	193	196	193	189	24

Table 5.15: Confusion matrix for classification by Maximum Likelihood classifier for test data

Classes	Pixels	Classified as							
		1	2	3	4	5	6	7	unclassified
1	498	456	0	0	0	0	0	0	42
2	1198	0	1040	0	39	43	0	1	75
3	769	0	0	698	13	0	0	0	58
4	747	0	41	24	657	0	0	2	23
5	503	0	3	0	0	457	0	1	42
6	695	0	0	0	0	13	636	0	46
7	498	0	0	0	14	11	0	442	31
Total	4908	456	1084	722	723	524	636	445	317

Table 5.16: Confusion matrix for classification by Backpropagation algorithm for test data

Classes	Pixels	Classified as							
		1	2	3	4	5	6	7	unclassified
1	498	493	0	0	0	0	5	0	0
2	1198	0	1021	39	33	0	0	0	105
3	769	0	0	684	19	0	0	0	66
4	747	0	5	0	668	4	0	0	70
5	503	0	0	2	17	468	0	1	15
6	695	0	0	0	14	3	626	1	51
7	498	0	21	0	4	0	0	467	6
Total	4908	493	1047	725	755	475	631	469	313

Table 5.17: Comparison of accuracy for different classes and total accuracy for different classifier

Classes	Training Data		Test Data	
	MLC (%)	BPL (%)	MLC (%)	BPL (%)
Water	99.0	94.0	91.6	98.9
Open Scrub Land	98.5	93.0	86.8	85.2
Salinity - I	96.5	93.0	90.8	88.9
Salinity - II	96.0	95.5	87.9	89.4
Crop	97.0	94.0	90.9	93.0
Mixed Urban	96.5	91.5	91.5	90.1
Vegetation	89.5	96.5	88.8	93.8
Total	96.14	93.93	89.76	91.32

Table 5.18: Area of different classes in classified images

Classes	Area (ha)	
	MLC	BPL
Water	90.02	114.45
Open Scrub Land	10682.45	10075.31
Salinity - I	1140.26	1237.58
Salinity - II	4200.96	5406.94
Crop	4020.92	4205.46
Mixed Urban	2010.46	2870.14
Vegetation	3000.69	3222.48
Unclassified	4861.11	2876.40
Total	30006.87	30006.87

Table 5.20: Table for comparison of each class by MLC and Backpropagation classifier

Classes in MLC	Pixels	Classified by Backpropagation							(%)
		1	2	3	4	5	6	7	
1	724	580	0	0	0	0	0	0	80.11
2	81293	0	55968	0	7349	8995	0	0	68.85
3	8762	0	0	5208	2347	0	0	0	59.44
4	31970	0	1398	177	25942	27	0	0	81.14
5	30600	0	62	0	20	21720	2167	0	70.98
6	15287	0	0	0	0	0	14739	254	96.42
7	22763	0	2353	0	0	2907	3798	13491	59.27
								Total	73.74

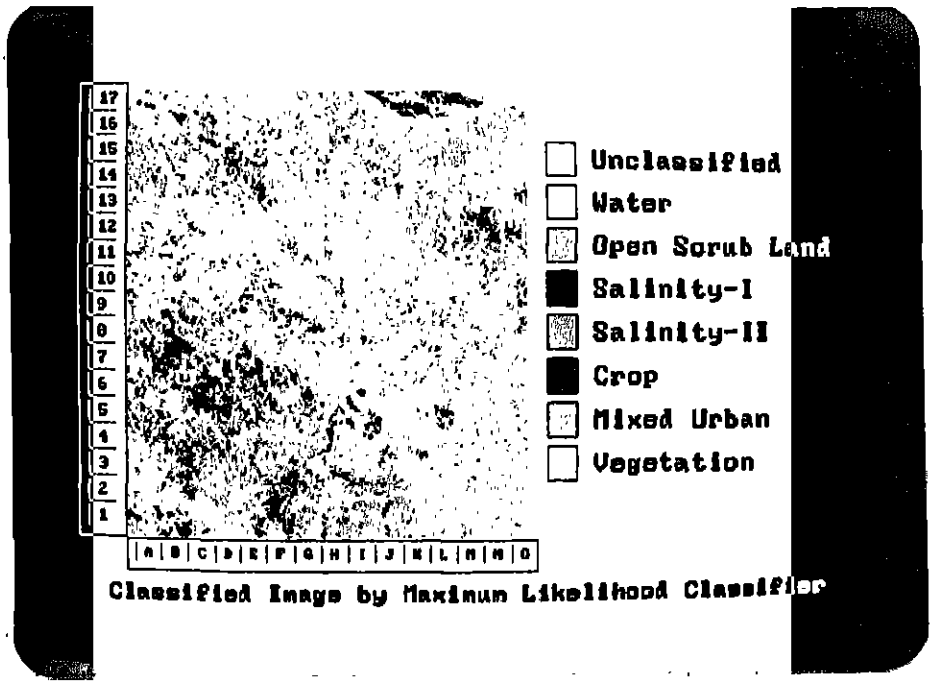

Figure 5.9: Classified Image by MLC

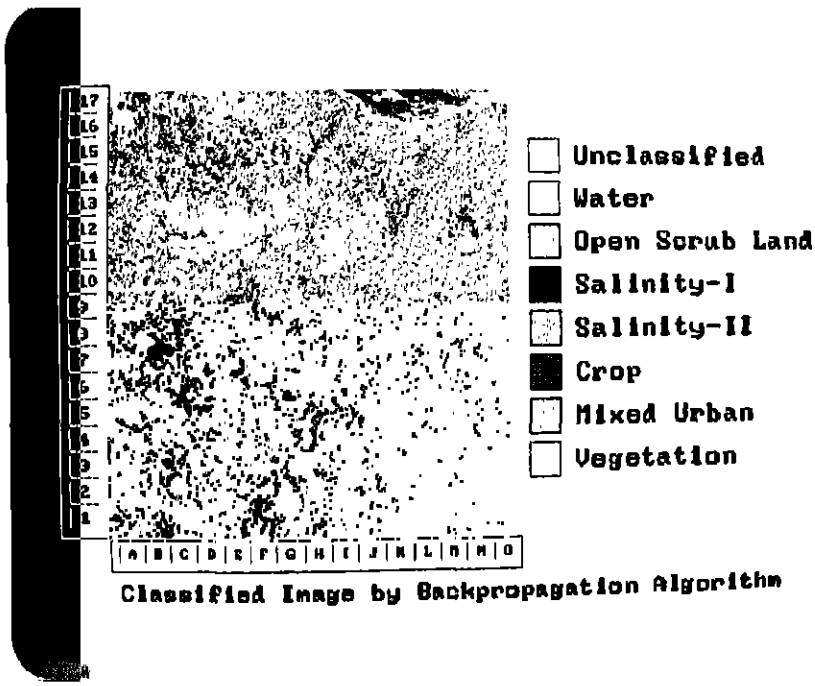

Figur 5.10 : Classified Image by BPL

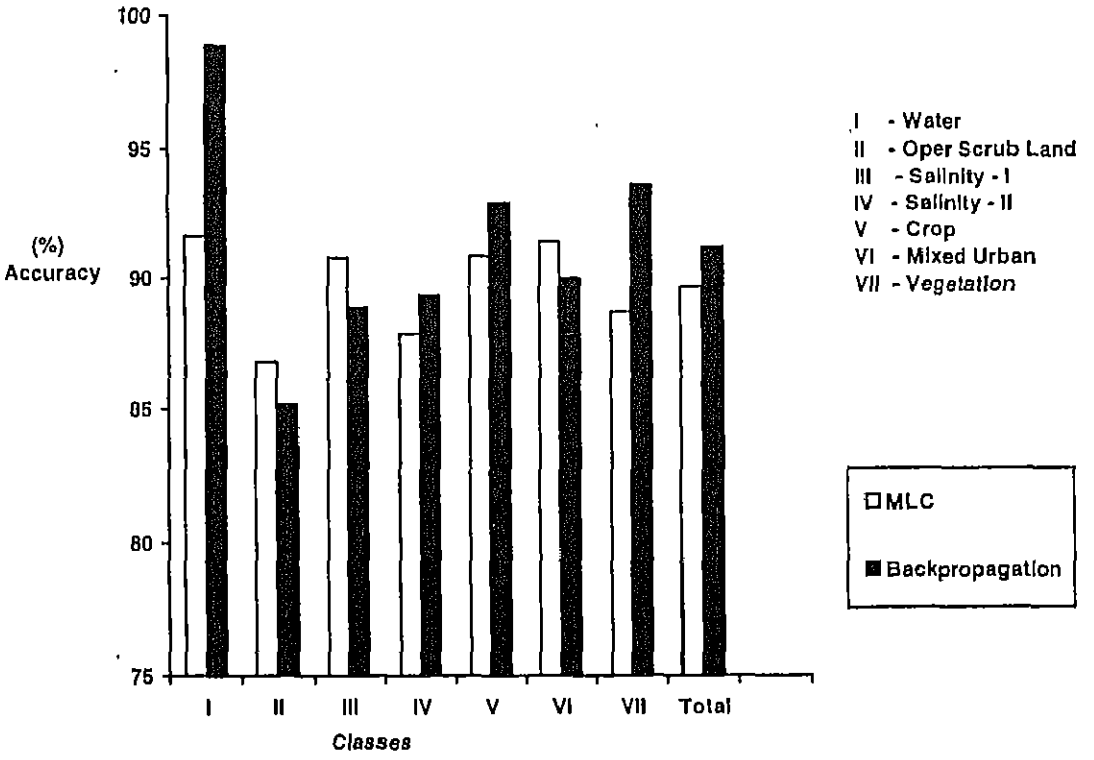

Figure 5.11 Comparison of accuracy of different classes for test data

CHAPTER 6

SOIL SALINITY USING GIS AND ANN

6.1 Introduction

Soil salinity is one of the major problem frequently observed in agricultural fields. It hampers the land use for both, agricultural purposes as well as for many civil engineering use. Salt affected soils cover an estimated 7 million hectare of India's total geographical area of 328 million hectares (Rao et. al. 1991, Dwivedi, 1992). Integration of Remote Sensing and GIS, providing near real time information with global coverage, can be very effective tool for the application of real time analysis. Extent of salinity may vary with season and it's spectral response also varies accordingly. Hence in present study, satellite data is obtained for two periods namely, November 1992 and April 1993 to demarcate changes in efflorescence of salts. For better delineation of the salt affected zones, the satellite data needs to be enhanced. Soil moisture and soil salinity are two major and to an extent, related concepts. Higher the moisture in the area higher is the probability of salinization in long terms. Modeling of variation in the spectral reflectance of the soil with and salinity is attempted. Based on the results of empirical models using satellite data and the information from digitally enhanced images, zones affected by salinity may be mapped. This will provide a global information on the concentration of salt present in different zones of the region. The techniques developed in present work will be useful to the field

engineers working for land hazard management by providing them data base regarding soil condition in the area. Since remote sensing data is repetitive in nature, it would be great use to monitor frequently the changes taking place in salinity level of the soil.

Usefulness of ANN has been established on conventional statistical classifiers in feature classification.. An attempt is made to apply ANN for salinity investigation. ANN holds the potential for identifying the salinity patches. They represent a fundamentally different approach to problem like pattern recognition, as they do not rely on statistical relationships. Instead, ANN adaptively estimate continuous functions from data without specifying mathematically how outputs depends on inputs.

The broad objective of this part of the study is to utilize remote sensing for delineating saline zones using artificial neural network and to model the spectral behavior of soil salinity taking into account both, ground field data and IRS-1B data. Investigation is targeted to

- investigate the spectral behavior of normal soil, saline soil and vegetation cover
- investigate the potential of artificial neural network classifier to detect the saline patches.
- study and analyze the salinity in soil and also developing empirical model to predict the same using IRS-1B data.
- estimate the change in salt affected area coverage between seasons using satellite digital data.

- quantitatively estimate the soil alkalinity using Geographical Information System.

6.2 Probable Cause of Salinity in the Region

Deposition of a layer of salt on top of soil surface is termed as Salinization. In present study area, over irrigation, frequent water logging, and high evaporation in the region, salt is transported through capillary action on the top of soil surface and deposited. This is a continuous phenomenon in a water logged area and in a long period of time, this accumulation leads to high concentration of these deposits and so problem of salinity. The study area affected by salinity is spread on both sides of lower Ganga canal. It also extends to far stretches due to large number of distributaries in the region. The soil in the area is sandy silt which is significantly porous and permeable in some regions. The percolation and infiltration of water to the ground is high because of the presence of these drains, most of which are generally unlined. Ground water table is quite high near the canal and decreases as we move away. The general level of ground water table is high and lies at a small depth from the surface. A large number of small channels dug in unplanned way by farmers has only multiplied the problem because of seepage and other losses.

6.3 Type of Soil Alkalinity

Soil salinity is due to sulphate and chloride salt of sodium and calcium. These salts are neutral salts and inactive with clay particles, it dilutes due to rain and other atmospheric

reasons with variation of season and second one, soil alkalinity it is due to carbonate and bicarbonate of sodium and calcium. These salts has formed a new clay structure. It changes the clay particle into permanent form and changes alkalinity with weather conditions. The study area mainly contains soil alkalinity having pH values 8 to 11. The area having pH values more than 10 has not potential to support any type of crop but soil having pH value less than 10 has possibility to change its concentration due rain and weather. This is main cause of change of soil alkalinity with seasons. The study area mainly contained loamy soil. The present study is an integrated approach to monitor the change in soil alkalinity using remote sensing and GIS.

6.4 Sampling Sites

The sampling sites are shown in Fig. 1.1 and details are given in Table 6.1. These sites has been identified through field survey and FCC of different seasons as shown in Figs. 5.1 and 6.1. These are selected such as to cover sites having well developed salts, affected but not visible on the surface, and normal soils. Samples are collected from ground surface as well as from certain depths. Proper care is taken in collected from ground surface as well as from certain depths and packing samples in order to preserve the *in situ* moisture. They are collected from some depths, as the top layer of the soil has negligible moisture does nor offer correct moisture of underneath soil. Soil samples collected from the field are tested for moisture content in the laboratory. Chemical tests are done to find alkalinity and chloride concentration.

6.5 Methodology

6.5.1 Soil moisture content

Soil samples collected at the ground surface have very negligible amount of moisture while those collected from certain depth have significant moisture. Results of moisture content determination is presented in Table 6.2. The moisture in the samples takes at certain depth varies from 6 to 20 percent. This clearly indicates that soil of the region has significant *in-situ* moisture. In the regions where salt has come on the ground, moisture content is low.

Table .6.1: Description of the sampling zones

Locations	Description of the site
1,2,6,19,20	Normal soils, These areas are in general have no significant effect of salt on the soils.
3,4,5,8,9,14,18	Soil moderately affected with salt, but the salt has not come above the ground at the time of sample collection.
7,10,11,12,13,15,17	The soil is severely affected by salt, salt can easily seen on the ground.

Thus it clearly indicates that large moisture coupled with high evaporation rate is a prominent cause of salinization in the region. The moisture content for moderately saline areas is little bit higher than highly saline soils but lower than those of normal soils

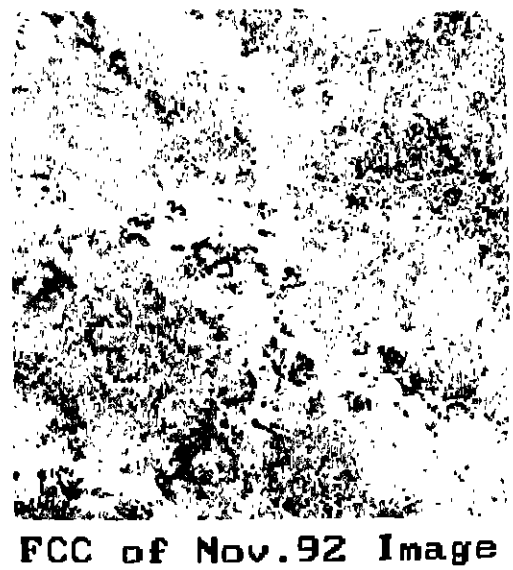

Figure 6.1 : FCC of November 1992

regions. The variation of moisture content in the region also justifies the variation in the spatial spread of saline zones.

6.5.2 Chemical analysis

Having a broad idea about the presence of various ions in salt from earlier works on Indo-Gangetic plains and other areas (Mougenot et. al., 1993, Rao et. al., 1991, Kalra et. al., 1994), chemical lab analysis is performed in the laboratory to alkalinity and chloride ions. Chemical analysis, generally requires a solution to test with for required parameters of the present study. Results of the chemical tests are presented in Table 6.2. The carbonates (CO_3^{-2}) and bicarbonates (HCO_3^{-1}) present in water mainly contribute to the alkalinity. The alkalinity is determined by titration.

6.6 Results of Laboratory Tests

The results of the chemical tests and moisture content determination are presented together in Table 6.2. The chemical analysis of the samples shows a typical trend. The salt samples generally shows higher values for various characteristics which decreases with the decrease in the effect and presence of salt in the soil. The chemical analysis of the saline samples has helped in identifying the presence of particular ions.

Table.6.2: Physical and Chemical properties of Soil Samples

Site No.	Moisture content (present)	pH	Alkalinity (mg/l as $CaCO_3$)	Chloride Concentration (mg/l)
1	15.60	9.00	190	Nil
2	19.40	8.60	115	Nil
3	17.00	9.50	550	3
4	12.20	9.70	910	3.6
5	19.80	8.50	90	Nil
6	9.40	10.95	1090	5.3
7	7.80	10.90	1300	6.0
8	11.00	10.40	1220	5.9
9	5.85	10.50	1120	6.1
10	20.10	9.40	300	2.5
11	14.67	9.40	770	2.2
12	6.54	11.00	1390	6.4
13	18.20	9.40	490	4.0
14	13.33	9.20	930	3.7
15	13.54	9.60	780	3.5
16	10.50	10.80	1310	5.8
17	13.00	9.50	930	3.6
18	13.73	9.10	780	3.2
19	16.41	8.50	150	Nil
20	17.5	8.20	120	Nil

Table.6.3: Grey level values and other parameter for sampling stations (Nov. 1992)

Site No.	Location	Row	Column	Grey level Values (band3)	Grey level Values (band4)	SI*100	Alkalinity (mg/l)
1	Abdulpur	245	341	46	47	98	190
2	Chandika	254	237	51	51	100	115
3	BadiPurwa 1	256	318	40	43	93	550
4	Badi Purwa 2	267	303	42	41	102	910
5	Gauri Lakha 1	269	212	37	36	102	1090
6	Gauri Lakha 2	251	206	37	48	77	1300
7	Gauri Lakha 3	232	201	32	38	84	1220
8	Bhagvantpur	229	214	30	39	77	1120
9	Laxmanpur	225	167	47	45	104	300
10	Jagatpur 1	240	133	40	40	100	770
11	Jagatpur 2	249	129	31	37	84	1390
12	Maharaj Nagar	281	128	48	47	102	490
13	Manoh Bari	299	139	39	43	91	930
14	Manoh Choti	310	149	47	48	99	780
15	Bhausana	319	173	35	36	80	1310
16	Dileep Nagar	332	204	40	44	90	930
17	Rautapur 1	324	248	44	42	98	780
18	Rautapur 2	295	269	52	48	108	150
19	Near Bridge on Sheoli Road	280	245	53	51	104	120

Table 6.4: Grey level values and other parameter for sampling stations (April, 1993)

Site No.	Location	Row	Column	Grey level Values (band3)	Grey level Values (band4)	SI*100	(NDSI +0.29) *600	Alkalinity (mg/l)
1	Abdulpur	245	341	42	68	62	30	190
2	Chandika	254	237	37	60	62	30	115
3	BadiPurwa 1	256	318	76	85	89	138	550
4	Badi Purwa 2	267	303	83	79	105	186	910
5	Champatpur	254	332	34	62	55	0	90
6	Gauri Lakha 1	269	212	110	85	131	252	1090
7	Gauri Lakha 2	251	206	96	82	117	222	1300
8	Gauri Lakha 3	232	201	102	80	128	246	1220
9	Bhagvantpur	229	214	78	79	99	168	1120
10	Laxmanpur	225	167	50	68	74	84	300
11	Jagatpur 1	240	133	86	81	106	156	770
12	Jagatpur 2	249	129	87	80	109	198	1390
13	Maharaj Nagar	281	128	70	82	85	126	490
14	Manoh Bari	299	139	85	74	115	216	930
15	Manoh Choti	310	149	96	88	109	198	780
16	Bhausana	319	173	92	82	112	186	1310
17	Dileep Nagar	332	204	92	83	111	204	930
18	Rautapur 1	324	248	70	68	103	180	780
19	Rautapur 2	295	269	38	68	56	6	150
20	Near Bridge on Sheoli Road	280	245	36	63	57	12	120

6.7 Digital Enhancement of Saline Zones

Digital image processing provides ample of scope to enhance the images to a particular level, where delineation of objects of interest becomes easier. In present study two new indices namely Salinity Index (SI) and Normalized Difference Salinity Index (NDSI) are proposed on spectral behavior of saline soil, which may have great potential in the identification of saline zones in the soil.

6.7.1 Digital smoothing

In this operation, image smoothing operations are required so as to eradicate noisy pixels. These pixels having high gray levels similar to saline patches may cause misinterpretation. At the same time, the care has to be taken to preserve the boundaries of saline patches. More precisely, the aim of digital filtering here is to eradicate spurious noise and preserve edges. The filters applied in the present work are : moving average and median filter. Moving average filter is excellent for random noise removal say due to backgrounds. The median filter which chooses window and search for median values of the included pixels and assigns it to central pixel. The output image thus received is smoother than the original one.

For any particular area being imaged, it is unlikely that the full dynamic range of the sensor is used. The corresponding image is dull and lacking in contrast. It is very difficult to

identify details on an under exposed image. Contrast stretching is done by the program **cont.c** to brighten up a dark image to make it more interpretable while maintaining the relative distribution of gray levels. Contrast stretching is based on the histogram of the original image. In present study *linear stretching* and *histogram equalization* is used.

6.7.2 Arithmetic Operation

Image Subtraction

The response of salts patches and saline zones is generally higher in band 3 and significantly lower in band 4 while that of vegetation and other related objects is higher in band 4 and lower in band 3. In this study, it has been tried to enhance the saline land features by subtracting images of two bands namely, red and near infrared of the same area. Image differencing is performed on pixel by pixel basis. The resulting image tends to have a histogram that is normal in shape. This procedure assists in the interpretation and understanding of an image in a better way. The mathematical expression is given as

$$GL_{i,j,r} = GL_{i,j,1} - GL_{i,j,k}$$

where

$GL_{i,j,r}$ = resultant digital number at position i,j

$GL_{i,j,1}$ = digital number at position i,j in band 1, and

$GL_{i,j,k}$ = digital number at position i,j in band k

Image Ratioing

Ratioing of two bands data enhance several features while suppresses some other features de[ending on the nature of the spectral reflectance curve of various features. A major advantage of the ratioed image is that it convey the spectral or color characteristics of image features, regardless of variations in scene illumination conditions. A ratioed image of scene effectively compensates for the gray level change caused by the varying topography and emphasizes the color content of the data. These clearly portray the variation in the slopes of spectral reflectance curve between two bands involved. The mathematical expression for the simple ratio is given as,

$$GL_{i,j,r} = GL_{i,j,l} / GL_{i,j,k}$$

Another most common operation, and even better in most of the cases, is normalized ratio. This is given as,

$$Gl_{i,j,r} = (Gl_{i,j,l} - Gl_{i,j,k}) / (Gl_{i,j,l} + GL_{i,j,k})$$

Salinity Index (SI) is the ratio of red band to near infrared band while Normalized Difference Salinity Index (NDSI) is the Ratio of the difference of the red to NIR and divided by the summation of the two. The concept originates from the Red Edge concept for vegetation vigor mapping. In Red Edge concept, the Spectral Reflectance of NIR is ratioed with Red band which gives very high value for vegetation than other features on Earth. Here if the inverse is taken in to consideration then for vegetation an equally low value will be obtained thus giving conceptual birth to SI and NDSI. Salinity Index and Normalized Difference Salinity Index are computed as follows :

$$SI = (Band\ 3 / Band\ 4) \times 100$$

$$NDSI = [(Band\ 3 - Band\ 4) / (Band\ 3 + Band\ 4)] \times 100$$

These are found particularly useful in the identification of the soil affected with salinity. SI is found to be superior in discriminating the saline zones. The values calculated for SI and NDSI for sampling stations are presented in Table 6.3 and 6.4 respectively. The red to NIR is typically very high in case of highly saline zones. NDSI has positive values for saline patches, high for highly saline and a low but, positive, for mildly affected patches. While in cases of vegetation, whether healthy and green to senescent, it is negative.

6.8 False Color Composites

The three band combination having the largest OIF is then selected for color composition because it should display the maximum information with the least amount of duplication as shown in Table 6.5. Often, three band combinations that are within two to three rankings of each other appear similar in color composite form because there is little difference in their information content. False color composites (FCC) is used through the program **fcc.c** to read information easily knowing behavior of different features. FCC is obtained by assigning bands in a particular order. This is important tool for visual interpretation of an area from remote sensing data. These composites are particularly helpful in differentiating the features.

Table . 6.5: Ranking of different band compositions based on OIF value

Rank	Bands	OIF value April	OIF value November
1	1 3 4	13.708	10.292
2	2 3 4	12.414	9.058
3	1 2 4	11.252	7.802
4	1 2 3	10.914	4.851

6.9 Empirical Models using Soil Alkalinity and Spectral Reflectance

The location map of the study area is digitized under ILWIS 1.41 environs using ALTEK Datatab digitizer (A0). This map is georeferenced using control points present in images of different bands and map. This procedure has yielded information about location of sampling point sources on satellite data. The corresponding reflectance of soil samples from different sampling zones are retrieved for different bands.

Empirical models for soil reflectance (SR) vs alkalinity, SI vs alkalinity and NDSI vs alkalinity has been prepared using regression analysis. It has been observed that a polynomial of second order yielded satisfactory results:

$$\text{Alkalinity (mg/l)} = a\rho^2 + b\rho + c$$

Where a, b, c are regression coefficients and ρ is the spectral reflectance / salinity index / normalized difference salinity index. The models have been prepared for November 1992

and April 1993 data. The regression coefficients thus obtained for each of the models are listed in Table 6.6

Table 6.6 : Regression parameter to empirical modeling

Month	Parameter	a	b	c	Coefficient of Correlation (%)
April 93	SR(band3)	-0.0774341	26.723	-764.525	79
April 93	SI	-0.04555	24.2837	-1125.57	85
April 93	NDSI	-0.000937	4.88441	71.5361	84
Nov.93	SR(band3)	-0.140401	-39.8994	2624.98	64
Nov.93	SI	-4947.95	5640.67	-111.749	66

It has been observed that empirical model of spectral reflectance using band 3 vs. alkalinity as shown in Fig. 6.2a has offered high coefficient of correlation 79 for April 1993 image. This empirical model for band 3 has been extended for whole image and alkalinity level is divided into six groups. The advantage of this model being generalized through GIS is that it directly gives the alkalinity levels at any desired point. The empirical models for SI vs. alkalinity and for NDSI vs. alkalinity shown in Figs. 6.2b and 6.2c on similar pattern have been developed. These empirical models have been applied on the complete area, which enhanced some new areas of high salinity and the same has been confirmed from field verification. The similar type of empirical models is generated for November 1992 image for observing the change in alkalinity level but it offered lesser coefficient of correlation for band 3 and for SI as shown Figs. 6.3a and 6.3b respectively. The NDSI model offered poor correlation in November and it has not been considered. The reason for the decrease

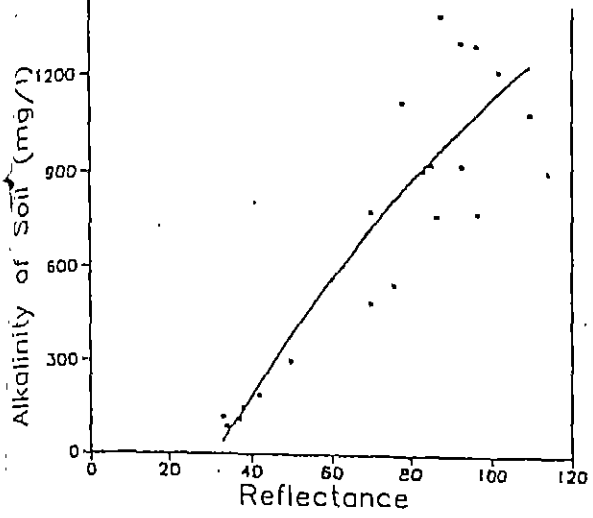

Figure 6. 2a

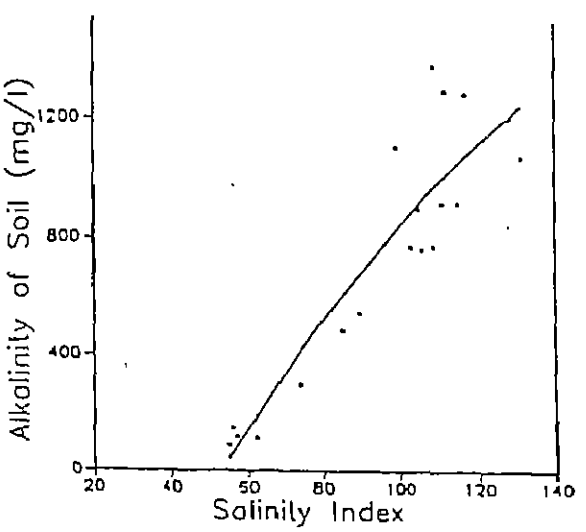

Figure 6.2b

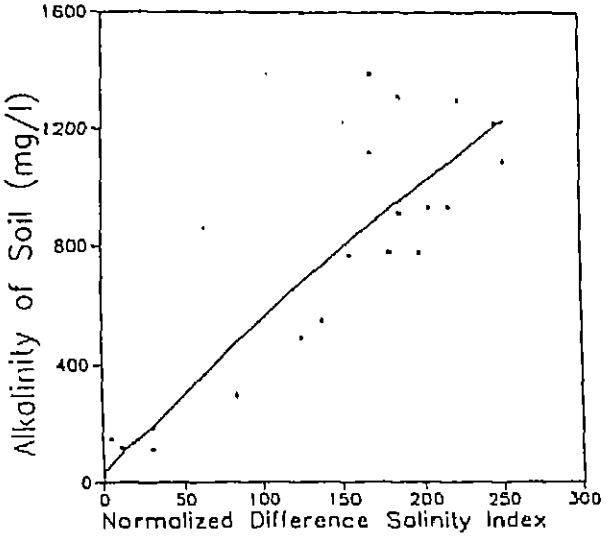

Figure 6.2c

Figure 6. 2a : Empirical relationship in Spectral Reflectance in Band 3 and Alkalinity for April 1993

Figure 6.2b : Empirical relationship in Salinity Index and Alkalinity for April 1993

Figure 6.2c Empirical relationship in Normalized Difference Salinity Index and Alkalinity for April 1993

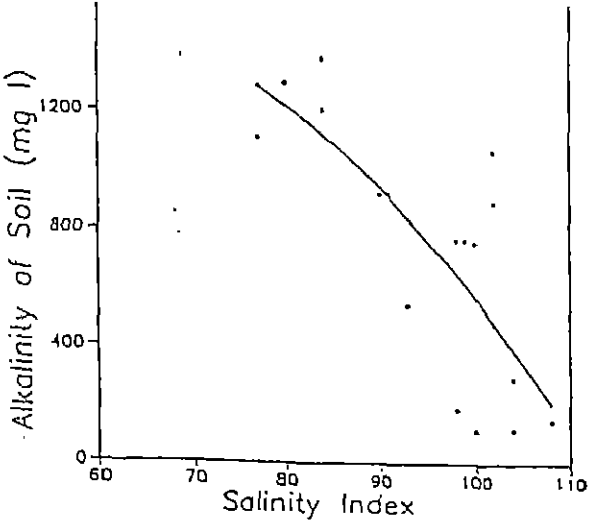

Figure 6.3a

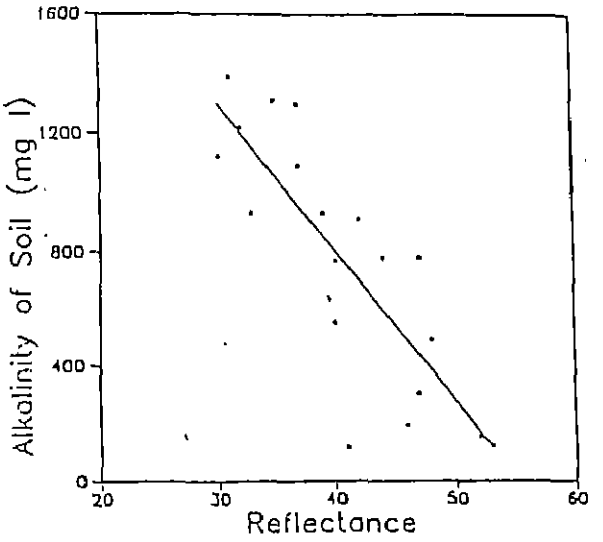

Figure 6.3b

Figure 6.3a : Empirical relationship in Spectral Reflectance in Band 3 and Alkalinity for November 1992

Figure 6.3b Empirical relationship in Salinity Index and Alkalinity for November 1992

in the alkalinity in November period is just because of dilution and washing of salt from the top of the surface due to rain. Due to this top few centimeters of the earth crust is devoid of the salt and farmers have been able to grow the paddy. In November the paddy crop is prolific and offers lesser scope to record soil signatures through satellite sensing. This may be a cause that the model for NDSI in November has yielded poor result.

6.10 Delineation of Salinity Zones using ANN

The usefulness of ANN as image classification is based upon several considerations. First, Backpropagation appears to yields better result than other neural techniques for identification of soil salinity patches and requires no assumptions such as normal distributions. Different salinity levels including high salinity zones that do not support any type of crop in any season have been extracted. The approach for both the study is same. From spatial modeling and ground survey it has been established that band - 3, SI and NDSI are giving best input for soil salinity. Three input vectors have been taken from band 3, SI and NDSI . The other parameters like learning rate, momentum factor and error were same as used in Chapter 5. The number of neurons in hidden layer has been calculated from Equation 5.3 and which is 5 for salinity level and 4 for very high salinity zones. For identification of salinity level the network has been trained for four classes. These four classes were low salinity, medium salinity, high salinity and river. The BPL network used for training is shown in Fig 6.4. The training network has converged and weights have adjusted. Image has been classified using above trained network and its

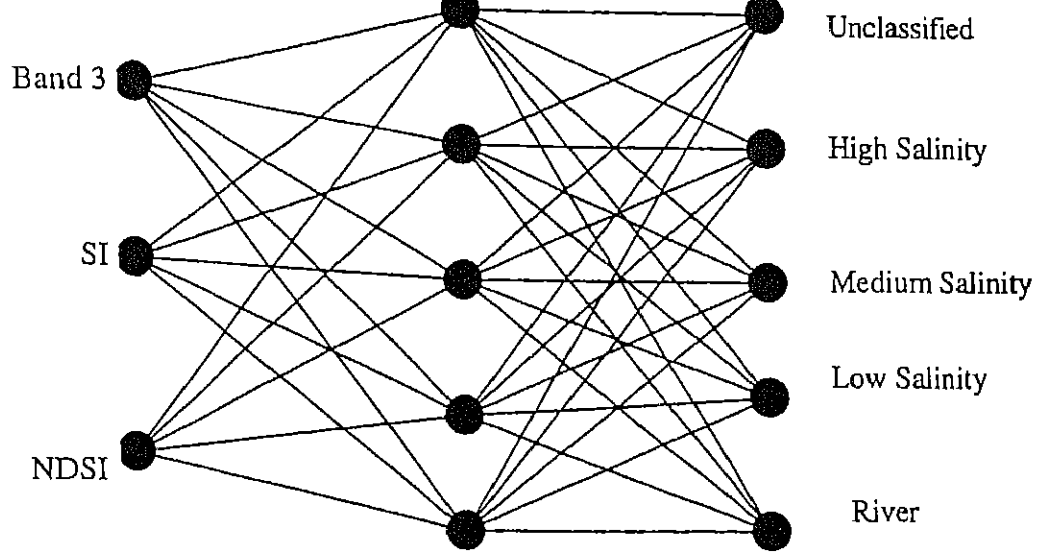

Figure 6.4: BP network for salinity level

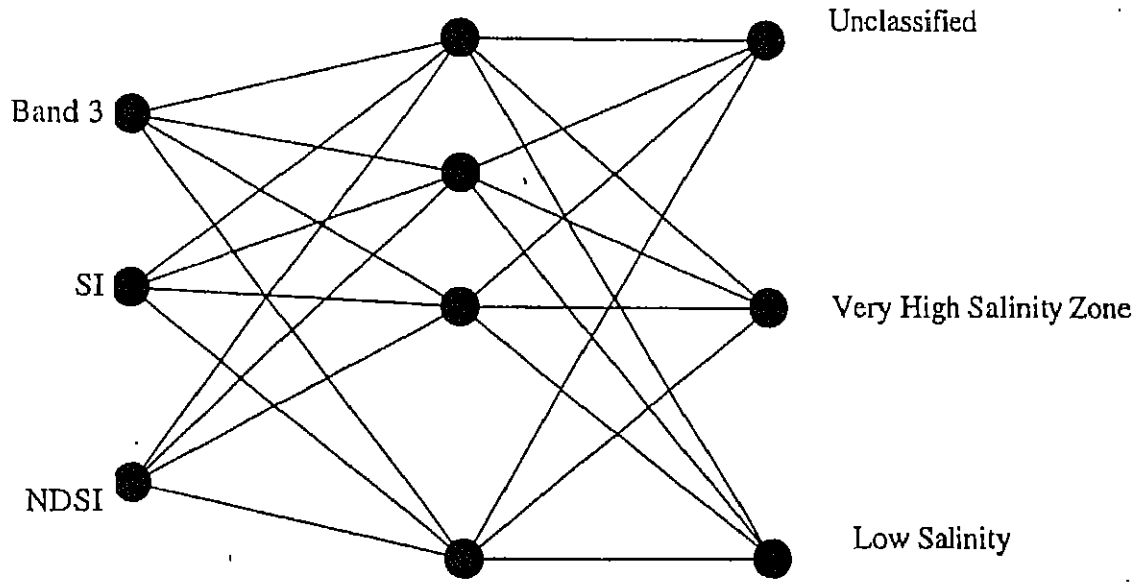

Figure 6.5: BP network for high salinity

result is presented in Fig. 6.9. The area of different salinity level is listed in Table 6.8. These areas are very close to area calculated by spatial modeling and available data in department of soil salinity at CSAU. This output image is showing unclassified pixels represented by black color. These represent mixed urban types.

The second approach was to identify the very high salinity zone, which are totally barren and absolutely useless for agriculture point of view. To identify these zones only two classes has been considered and output are obtained using similar procedure as discussed above. The BPL network used for training is shown in Fig. 6.5 and the classified image is shown in Fig. 6.10. The area calculated for very high salinity zone is 2100.48 ha. In this classified image, there are few patches near D-12, D-13, E-12, E-13 as unclassified pixels. These are vegetation and forest type area as identified in Figs 5.10.

6.11 Zones of Salinity in the Region

From FCC, shown in Fig 5.1, *SI* image, *NDSI* image and classified image of April 1993, it is evidenced that the biggest saline zone of the area occur between Pandu nadi and Lower Ganga Canal (Kanpur branch) . These patches can be seen in different salinity maps from Figs. 6.6 to 6.8. The empirical models generated have been used in spatial modeling and images of alkalinity have been generated for April 1993. Whole area is divided into different zones for different approach and it is given in Table 6.7 and 6.8 The area covered under very. high salinity are causing main problem in the regionTable 6.7 presents the areas covered by different zones of salinity of IRS-1B April image of the region.

Table 6.7 : Area of different saline zones using different empirical models of IRS-1B data

Class	Level (Alkalinity)	Area (ha) in Nov. 92		Area (ha) in April 93		
		Band 3	SI	Band 3	SI	NDSI
0	Others	3180.0114	3254.7780	885.7674	901.7982	895.8852
1	V.Low	10379.9430	8970.6780	3621.1212	3304.9728	3414.2976
2	Low	9279.8622	9960.6456	9151.4844	8173.3428	7888.2048
3	Medium	5527.7352	5965.6914	9018.3762	9217.71	9869.9796
4	High	1469.0520	1636.7184	5548.6278	6081.7176	5322.0942
5	V. High	168.8490	216.9414	1780.0758	2325.9114	2614.9914

Table 6.7: Area of different salinity zone by ANN

S. No.	Classes	Area (ha)
1	High Salinity	1987.63
2	Medium Salinity	5063.28
3	Low Salinity	15490.8
4	River	113.48

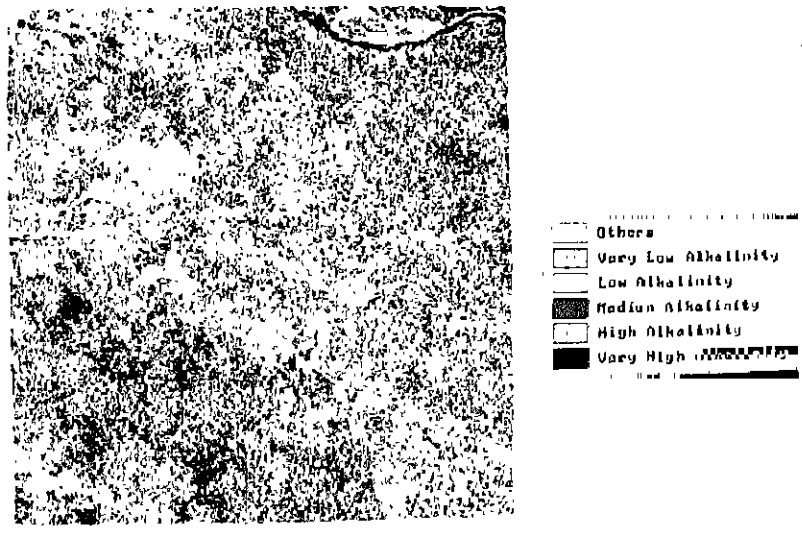

Figure 6.6 Alkalinity map of band 3

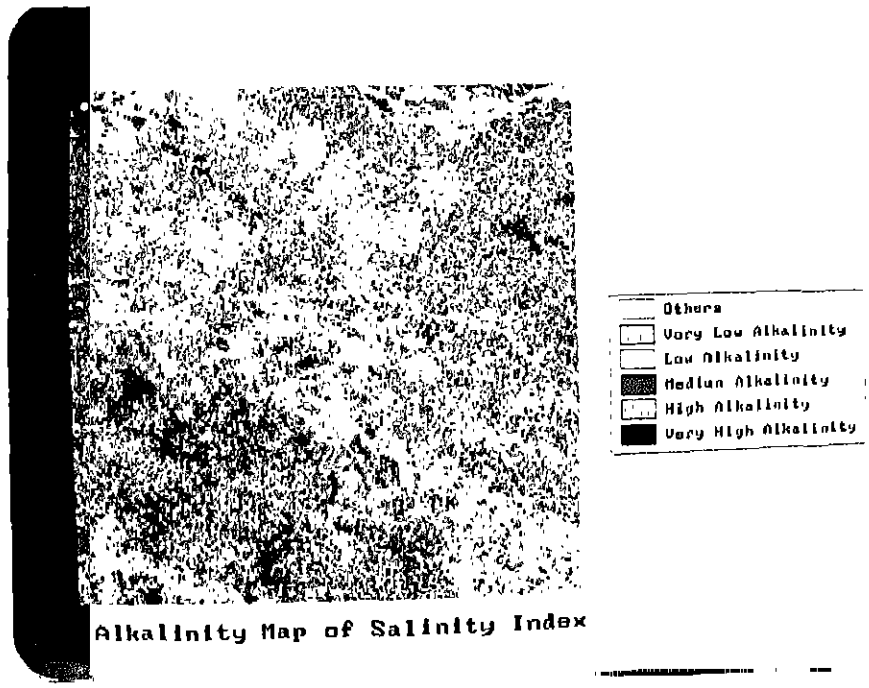

Figure 6.7 Alkalinity map of SI

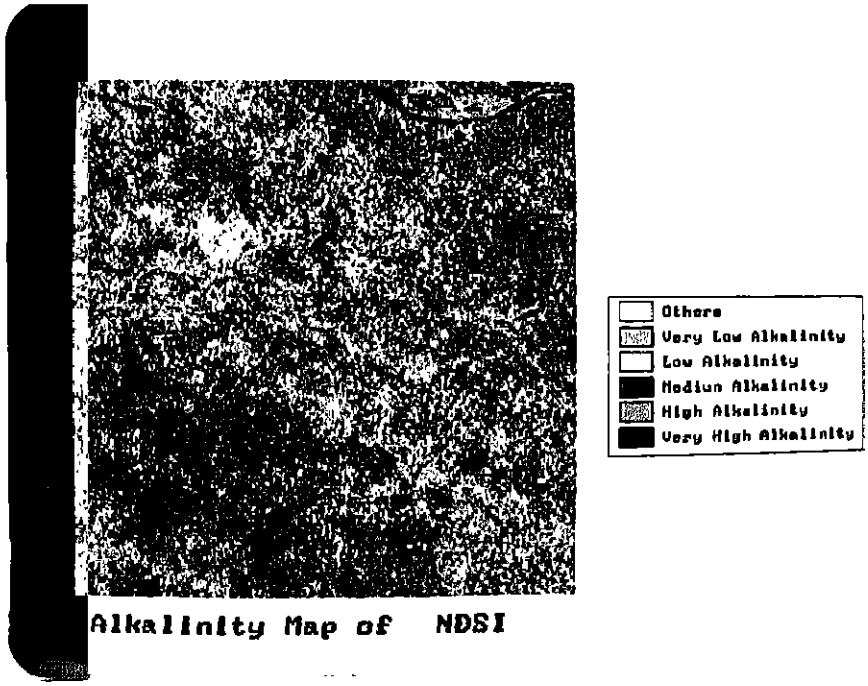

Figure 6.8: Alkalinity map of NDSI

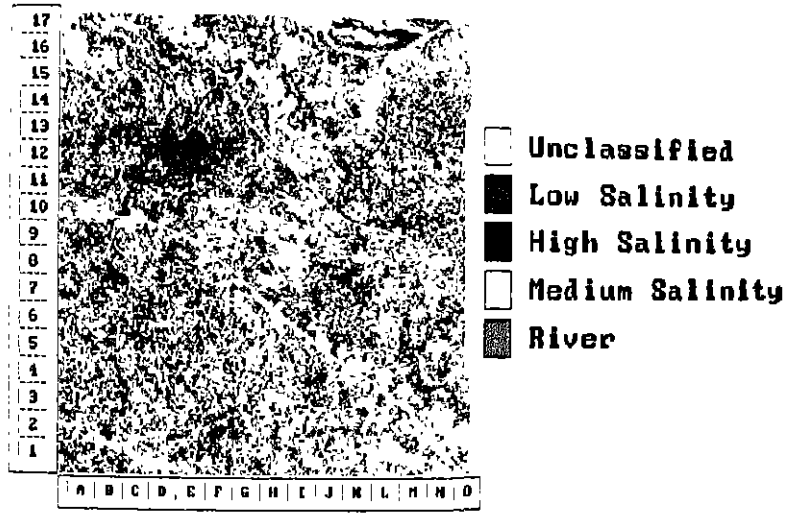

Figure 6.9: Salinity level using ANN

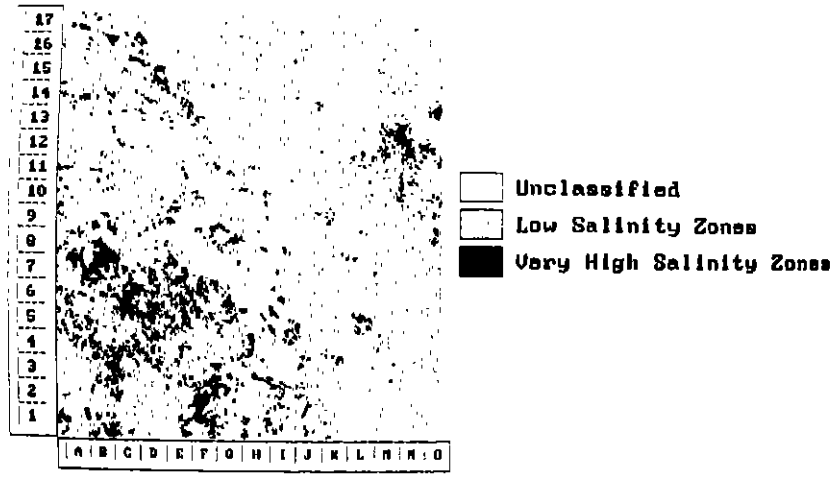

Figure 6.10 Very high salinity zones

6.12 Conclusions

Result of this study mark following conclusions:

- Remote Sensing data in GIS environs may yield very useful database of soil alkalinity.
- SI and NDSI yield better result for April 1993.
- Neural Network classifier has potential to detect the salinity patches.
- Median filtering prior to image analysis is useful to minimize misinterpretation.
- Five zones of salinity observed in the study regions.
- The alkalinity levels of each point and various region along with area estimation is possible in GIS environment.

CHAPTER 7

CONCLUSIONS AND FUTURE RECOMMENDATIONS

7.1 Conclusions

The present study has presented a comparative appraisal of unsupervised statistical classifiers with ANN. A *case study for application of ANN in salinity estimation* is also explored. Remotely sensed data have been utilized in GIS environment of ILWIS 1.41 alongwith field data. The results obtained are also compared with results of ANN for salinity determination. Conclusion drawn from present work are listed below:

- The SOFM (Kohonen's algorithm) offers good classification for some classes like crop and water but totally failed in soil salinity and mixed urban. The overall accuracy of SOFM is poorer than unsupervised clustering (UC).

- Backpropagation Learning (BPL) yielded better result than SOFM, UC and MLC and its potential lies in case of small training data. The BPL approach to neural network training is extremely computational intensive, taking considerable time in training but lesser time in classification. The overall accuracy is 91.32 percent in case of BPL and 89.76 percent in case of MLC. This difference is much higher in case of small training set. The overall accuracy is 67.4 percent in case of BPL and 49.4 percent for MLC using 25 training pixels.

- BPL has proved its potential in identifying different levels of salinity zones. The approach used in this study by proposing SI and NDSI has offered very good result. This helped in better delineation of soil salinity with other surrounding features.

- Remote Sensing data analysis with field sample data in GIS environs have yielded very useful spatial database of soil alkalinity for the study region.

Overall conclusion of the study is that ANN approach using Backpropagation Learning has proved to be a very powerful tool for feature classification. It takes large chunk of time in training but works very fast for classification. It has also proved to be useful in generating the soil salinity database of the study region without going through the rigorous process of conventional digitization, spatial modelling and analysis in GIS environment. It certainly can help in minimising the cost and time involved and offer an alternate to conventional approach.

7.2 Future Recommendations

The study has provided several points which need to be taken care to make the algorithm faster thus reducing the time involved in training the BPL. Sigmoid function has been used in present case. Several other popular activation functions are available, which may be tried to investigate their response. Kohonen SOFM did not yield good result but a multispectral approach may offer better result. These issues may be tackled in future.

REFERENCES

Abuelgasim, Abdelgadir A., Sucharita Gopal, James R. Irons and Alan H. Strahler, 1996. Classification of ASAS multiangle and multispectral measurements using artificial neural network, *Remote Sensing Environmental*, 57:79-87.

Aminzadeh, Fred, Simon Katz and Keiti Aki, 1994. Adaptive neural nets for generation of artificial earthquake precursors, *IEEE Transactions on Geoscience and Remote Sensing*, 32(6): 1139 - 1143.

Anand, Rangachari Anand, Kishan G. Mehrotra, Chilukuri K. Mohan and Sanjay Ranka, 1993. An improved algorithm for neural network classification of imbalanced training sets,*IEEE Transactions on Neural Networks*,4(6): 962 - 969.

Arabshahi, Payman, Jai J. Chai, Robert J. Marks II and Thomas P. Caudell, March 1996. Fuzzy Parameter adaptation in optimization, *IEEE computational Science and Engineering*.

Arenz, R. F., Tr. W. M. Lewis Tr. and J. F. Saunders, III, 1996. Determination of chlorophyll and dissolved organic carban from reflectance data for colorado reservoir. *International J. Remote Sensing*, 17(8):1547-1566.

Augusteijn, Marijke F., Laura E. Clanens and Kelly A. Shaw, 1995. Performance evaluation of texture measures for ground cover identification in satellite images by means of a neural network classifiers, *IEEE Transactions on Geoscience and Remote Sensing*, 33(3):616 - 626.

Baraldi, Andrea and Flavio Parmiggiani, 1995. A neural network for unsupervised categorization of multivalued input pattern: An application to satellite image clustering, *IEEE Transactions on Geoscience and Remote Sensing*, 33(2):305 - 316.

Belward, Alan S., and Carlos R. Valenzuela, 1990. Remote sensing and Geographical Information Systems for resource management in developing countries, Euro Course.

Benediktssen, Jan. A., Philip H. Swain and Okan K. Ersay, 1990. Neural network approaches verses statistical methods in classification of multisource remote sensing data, *IEEE Transactions on Geoscience and Remote Sensing*, 28(4): 540 - 552.

Benediktsson, J. A., P. H. Swain and O. K. Ersoy, 1993. Conjugate gradient neural networks in classification of multisource and very high dimensional remote sensing data, *International J. Remote Sensing*, 14(15): 2883-2903.

Bolstad, Paul V. and T. M. Lillesand, 1991. Rapid maximum likelihood classification, *Photogrammetric Engineering & Remote Sensing*, 57(1):67-74.

Carpenter, Gail A., and Stephen Grossberg, 1988. The ART of adaptive pattern recognition by a self - organizing neural network, *Computer*.

Clark, C. and A. Comas, 1995. Spectral identification by artificial neural network and genetic algorithm, *International J. Remote Sensing*, 16(12):2255-2275.

Cybenko, George, Dartmonth College, March 1996. Neural networks in computational science and engineering, *IEEE Computational Science and Engineering*,.

Davis, T. Daviel, Zhengxias Chen, Leung Tsang, Jenq-Nung Hwang and Alfred T. C. Chang, 1993. Retrieval of snow parameters by herative inversion of a neural network, *IEEE Transactions on Geoscience and Remote Sensing*, 31(4):843 - 851.

Dikshit, O., 1992. The classification of texture in remotely - sensed environmental imagery, Ph. d. Thesis, University of Cambridge.

Dreyer, Peter, 1993. Classification of land cover using optimized neural nets on SPOT data. . *Photogrammetric Engineering & Remote Sensing*, 59(5):617-621.

Dwivedi, R. S., 1992. Monitoring and the study of the effects of image scale on delineation of salt affected soils in the Indo-Gangetic plains, *International J. Remote Sensing*, 13(8):1527-1536.

Dwivedi, R. S., and Rao, B. R. M., 1992. The Selection of best possible Landsat-TM band combination for delineating salt affected soils, *International J. Remote Sensing*, 13(11):2051-2058.

Dwivedi, Praveen, 1995. Determination of salinity and its extent using digital remotely sensed data in Indo-Gangetic alluvial plains near Kanpur, M. Tech. Thesis, I.I.T. Kanpur.

Ersay, Okan K., and Daesik Hang, June 1990. Parallel, self - organizating, hierarchical neural networks, *IEEE Transactions on Neural Networks*, 1(2).

Foody, Giles M.,1996. Relating the long cover composition of mixed pixels to artificial neural network classification output, *Photogrammetric Engineering & Remote Sensing*, 62(5):491-499.

Foody, Giles M., Mary B. McCulloch and Willian B. Yates, 1995. Classification of remotely sensed data by an artificial neural network: issuses related to training data characteristics, *Photogrammetric Engineering & Remote Sensing*, 61(4): 391 - 401.

Foody, G. M., 1995. Using prior knowledge in artificial neural network classification with a minimal training set, *International J. Remote Sensing*, 16(2):301-312.

Foody, G. M., M. B. Meculloch and W. B. Yates, 1995. The effect of training set size and composition on artificial neural network classification, *International J. Remote Sensing*, 16(9):1707-1723.

Gang, P., 1996. Integrated analysis of spatial data from multiple sources using evidential reasoning and artificial neural network techniques for geological mapping. *Photogrammetric Engineering & Remote Sensing*,62(5): 513-523.

Gopal, Sucharita and Curtis Woodcock, 1996. Remote sensing of forest change using ANN, *IEEE Transactions on Geoscience and Remote Sensing*, 34(2):234-244

Hara, Yoshihisa, Robert G. Atkins, Simen H. Yuch, Robert T. Shin and J. A. Kang, 1994. Application of neural networks to radar image classification, *IEEE Transactions on Geoscience and Remote Sensing*, 32(1): 100 - 109.

Hepner, George F., Thomas Logan, Niles Ritter and Nevin Bryant, 1990. Artificial neural network classification using a minimal training set: comparison to conventional supervised classification. *Photogrammetric Engineering & Remote Sensing*, 56(4):469 - 473.

Jain, Anil K., Jianchang Mao and K. M. Mohinddin, March 1996. Artificial neural networks, *Computer*.

Joshi, Anupam, Sanjiva Weerawarana, Narendra Ramakrishnan, Elias N. Houstis and John R. Rice, March 1996. Neuro - Fuzzy support for problem solving environments - A step toward automated solution of PDEs, *IEEE Computational Science and Engineering*.

Kangas, Jari A., Teuvo K. Kohnen and Jorma T. Laoksonen, 1990. Variants of self organizing maps, *IEEE Transactions on Neural Networks*,4(1):93-110.

Key, J., J. A. Maslanik and A. J. Schweiger, 1989. Classification of merged AVHRR and SMMR arctic data with neural networks, *Photogrammetric Engineering & Remote Sensing*, 55(9):1331-1338.

Kim, H. Y. and Hyun S. Yang, 1991. Efficient image labelling based on markov random field and error backpropagation network, *Pattern Recognition*, 26(11):1695-1707.

Koh, Jean, Minsoo Suk and Suchendra M. Bhandarkar, 1995. A multilayer self organizing feature map for range image segmentation, *Neural Networks*, 8(1): 67 - 86.

Lee, Janathan, Ronald C. Weger, Sailes K. Sengupta and Ronald M. Welch, 1990. A neural network approach to cloud classification, *IEEE Transactions on Geoscience and Remote Sensing*, 28(5):847 - 855.

Lillesand, T. M. and Kiefer, R. W. , 1994. Remote sensing and image interpretation, John Wiley and Sons, Inc.

Lippmann, Richard P., 1987. An introduction to computing with neural network, *IEEE ASSP Magazine.*

Liu, Z. K. and J. Y. Xiao, 1991. Classification of remotely sensed image data using artificial neural networks, *International J. Remote Sensing*, 12(11):2433-2438.

Lu, Siwei and Anthany Szeto, 1993. Hierarchical artificial neural networks for edge enhancement, *Pattern Recognition*, 26(8): 1149-1163.

Mather, P. M., 1987. Computer processing of remotely sensed images, Wiley & Sons, Inc.

Mckeown, David M., 1987. The role of artificial intelligence in the integration of remotely sensed data with GIS, *IEEE Transactions on Geoscience and Remote Sensing*, 25(3):330-348.

Musavi, M. T., K. H. Chan, D. M. Hummels and K. Kalantri, 1994. On the generalization ability of neural network classifiers, *Transaction of Pattern analysis & Machine intelligence*, 16(6): 659 - 663.

Needeljkovic, Vladimir, 1993. A novel multilayer neural networks training algorithm that minimizes the probability of classification error. *IEEE Transactions on Neural Networks*,4(4): 650 - 659.

Niblack, W. , 1986. Digital image processing, PHI international.

Pal, Nikhil R., James C. Bezdek and Eric C. K. Tsaa,1993. Generalized clustering networks and kohonen's self - organizating scheme, *IEEE transaction on neural networks*, 4(4): 549-557.

Paola, Justin D. and Robert A. Schowengerds, 1995. A detailed comparison of backpropagation neural network and maximum likehood classifiers for urban land use classification, *IEEE Transactions on Geoscience and Remote Sensing*, 33(4): 981 - 996.

Rao, B. R. M., R. S. Dwivedi, L. Venkataratnam, T. Ravishankar, S. S. Thammappa, G. P. Bhargawa, and A. N. Singh, 1991. Mapping the magnitude of Sodicity in part of the Indo-Gangetic plains of Uttar Pradesh, Northern India using Landsat - TM data, *International J. Remote Sensing*, 12(3):419 - 425.

Richards, J. A. , 1986 Remote sensing digital image analysis, Springer and Verlag.

Salu, Yehuda and James Tilton, 1993. Classification of multispectral image data by the binary diamond neural network and by nonparametric, pixel - by - pixel methods, *IEEE Transactions on Geoscience and Remote Sensing*, 31(3): 606 - 617.

Sehaale, M. and R. Furrer, 1995. Land surface classification by neural networks, *International J. Remote Sensing*, 16(16): 3003-3031.

Setiono, Rudy and Huan Liu, March 1996. Symbolic Representation of neural networks. *Computer*.

T., Kohonen, 1984. Self organisation and adaptive memory, Springer Verley, Berlin.

Tan, Chew Lim, Tang sung Quah and Hoon Heng The, March 1996. An artificial neural network that models human decision making, *Computer*.

Tsang, Leung, Zhengxiao Chan, Seho oh, Robert J. Marks II and A. T. C. Chang, 1992. Inversion of snow parameters from passive microwave remote rensing measurements by a neural network trained with a multiple scattering model, *IEEE Transactions on Geoscience and Remote Sensing*, 30(5): 1015 - 1024.

Tzeng, Yu Chang, K. S. Chen, Wen Liang Rao and A. K. Fung, 1994. A dynamic learning neural network for remote sensing applications, *IEEE Transactions on Geoscience and Remote Sensing*, 32(5):1096 - 1102.

Xia, Li, 1996. A method to improve classification with shape information, *International J. Remote Sensing*, 17(8): 1473-1481.

Yoshida, Tomoji and Sigeru Omatu, 1994. Neural networks approach to land cover mapping, *IEEE Transactions on Geoscience and Remote Sensing*, 32(5):1103 - 1109.

Wesserman, P. D. , 1989. Neural Computing: Theory and practice, Van Nostrand Reinhold, New York.

APPENDIX - A

List of important Computer Programs developed for thesis

Programs for supervised classification using Back-Propagation algorithm

trn_sig_ext.c :- Program uses this GT file to extract the training data set from the input images.

ann_trainer.c :- Program uses this reshuffled training data set to train the multilayer perceptron model.

con_mat_gen.c :- Program classified the training data set to assess the performance of the classifier is done through the program.

ann_classifier.c :- Program classified the actual images using the trained binary network file.

Programs for unsupervised classification using Self-Organising Kohonen algorithm

input.c :- Program uses to read input file in required format.

node.c :- Program uses to define the output node of classified image.

SelfOrg.c :- Program classified the input image.

output.c :- Program uses to store the classified image from SelfOrg.c.

extract.c :- Program extracts the unsupervised classified image from output.c.

Programs for general image processing operations

scale1.c :- Linear contrast stretching program.

scale.c :- Linear contrast stretching using different look up table.

dis1.c :- Program to display the original image in gray shade.

dis.c :- An image display program using different lookup table.

fcc.c :- Program to display the false color composite.

cont.c	:-	Program to display the image after contrast stretching.
his.c	:-	To display the image after histogram equalization.

Programs for supervised classification using Maximum-Likelihood algorithm

send.c	:-	This program displays the image and mouse activated with the image that helps in training the data, all required data stored in a file.
inverse.c	:-	This is a simulation program for calculation of inverse of matrix and means etc. and called many times in maximum likelihood program.
max_like.c	:-	A supervised classification program using maximum liklelihood algorithm.
simutils.c	:-	This program is called many times in maximum likelihood program and useful for matrix operation.

123313

Date Slip 123313

This book is to be returned on the date last stamped.

CE-1997-M-RA1-501